ELSEVIER

Clinical Neurophysiology 113 (2002) 206–226

www.elsevier.com/locate/clinph

Trial-to-trial variability of cortical evoked responses: implications for the analysis of functional connectivity

Wilson A. Truccolo[a], Mingzhou Ding[a], Kevin H. Knuth[b], Richard Nakamura[c], Steven L. Bressler[a,*]

[a]*Center for Complex Systems and Brain Sciences, Florida Atlantic University, 777 Glades Road, Boca Raton, FL, 33431, USA*
[b]*Center for Advanced Brain Imaging and Cognitive Neuroscience and Schizophrenia Department, Nathan Kline Institute, Orangeburg, NY, 10962, USA*
[c]*Laboratory of Neuropsychology, National Institutes of Mental Health, Bethesda, MD, 20892, USA*

Accepted 7 December 2001

Abstract

Objectives: The time series of single trial cortical evoked potentials typically have a random appearance, and their trial-to-trial variability is commonly explained by a model in which random ongoing background noise activity is linearly combined with a stereotyped evoked response. In this paper, we demonstrate that more realistic models, incorporating amplitude and latency variability of the evoked response itself, can explain statistical properties of cortical potentials that have often been attributed to stimulus-related changes in functional connectivity or other intrinsic neural parameters.

Methods: Implications of trial-to-trial evoked potential variability for variance, power spectrum, and interdependence measures like cross-correlation and spectral coherence, are first derived analytically. These implications are then illustrated using model simulations and verified experimentally by the analysis of intracortical local field potentials recorded from monkeys performing a visual pattern discrimination task. To further investigate the effects of trial-to-trial variability on the aforementioned statistical measures, a Bayesian inference technique is used to separate single-trial evoked responses from the ongoing background activity.

Results: We show that, when the average event-related potential (AERP) is subtracted from single-trial local field potential time series, a stimulus phase-locked component remains in the residual time series, in stark contrast to the assumption of the common model that no such phase-locked component should exist. Two main consequences of this observation are demonstrated for statistical measures that are computed on the residual time series. First, even though the AERP has been subtracted, the power spectral density, computed as a function of time with a short sliding window, can nonetheless show signs of modulation by the AERP waveform. Second, if the residual time series of two channels co-vary, then their cross-correlation and spectral coherence time functions can also be modulated according to the shape of the AERP waveform. Bayesian estimation of single-trial evoked responses provides further proof that these time-dependent statistical changes are due to remnants of the evoked phase-locked component in the residual time series.

Conclusions: Because trial-to-trial variability of the evoked response is commonly ignored as a contributing factor in evoked potential studies, stimulus-related modulations of power spectral density, cross-correlation, and spectral coherence measures is often attributed to dynamic changes of the connectivity within and among neural populations. This work demonstrates that trial-to-trial variability of the evoked response must be considered as a possible explanation of such modulation.

Keywords: Cerebral cortex; Event-related potential; Evoked response variability; Effective connectivity; Correlation; Coherence

1. Introduction

A number of cerebral cortical functions are thought to involve transient task-dependent changes in the functional interdependence of neurons in the same and/or different cortical areas. Examples include perceptual binding and segmentation (Gray, 1999; von der Malsburg, 1994), multimodal integration (Bressler, 1995, 1996; Damasio 1989a,b; Sporns et al., 1994; Tononi et al., 1992), and selective attention (Olshausen et al., 1993). Generally, evidence for such changes purportedly comes from stimulus- or task-related modulation of statistical interdependence measures, such as cross-correlation or spectral coherence, that are derived from various types of cortical recordings. In addition, changes in the level of interaction within a neuronal population are inferred from temporal modulation of the power spectral density of population signals such as the local

* Corresponding author. Tel.: +1-561-297-2230; fax: +1-561-297-3634.
E-mail address: bressler@fau.edu (S.L. Bressler).

1388-2457/02/$ - see front matter
CLINPH 2001102
PII: S1388-2457(01)00739-8

field potential (LFP) or electroencephalogram (EEG) (Fries et al., 2001; Kalcher and Pfurtscheller, 1995; Pfurtscheller and Lopes da Silva, 1999). Indeed, recent studies have provided evidence for the event-related modulation of all these statistical measures in a number of different experimental preparations. Such modulation is usually understood in terms of changes in the level of synchrony of neuronal pulse activity. Fast transient changes in functional connectivity of the underlying neural circuitry (i.e. changes in synaptic efficacy and/or effective connectivity occurring on time scales of $\sim$100 ms) are often identified as the sources of such events (Aertsen et al., 1994, 1989; Bressler et al., 1993; Buchel and Friston, 1997; Chawla et al., 1999b; Gray et al., 1989; Rodriguez et al., 1999; Srinivasan et al., 1999; Tallon-Baudry et al., 1997, 1998).

In this paper, we show that temporal modulation of power and interdependence measures may result from *trial-to-trial* non-stationarity of the cortical evoked response. Trial-to-trial variability in amplitude, latency and waveform of the evoked response constitute manifestations of this non-stationarity (Coppola et al., 1978; Lange et al., 1997; Mocks et al., 1987; Pham et al., 1987). We demonstrate that trial-to-trial variability in the amplitude and latency of evoked local field potentials, can, in the appropriate context, lead to temporal modulation of the aforementioned statistical measures, producing effects that could resemble either transient synchronization or, alternatively, transient desynchronization events. Consequently, inter-trial variability of the evoked response may appear as *intra-trial* stimulus- or task-related modulation of intrinsic parameters in the neural system. To overlook this possibility, as is commonly done, may result in the erroneous interpretation of trial-to-trial non-stationarity as *intra-trial* task-related changes in functional connectivity.

In order to understand the effect of trial-to-trial amplitude and latency variation on interdependence measures, we reconsider the long-standing question of how to model the cortical potentials that follow presentation of a sensory stimulus. At least since the time of Dawson (1954), the most common model of the post-stimulus cortical potential postulates that a single trial waveform is the linear combination of an invariant stimulus phase-locked evoked component (signal) and an ongoing background noise component. The evoked response component is treated as being time-invariant since any changes over trials in its amplitude, latency onset, or waveform are considered to be negligible. The usual method of measuring this component is to repeatedly present the same sensory stimulus and then average the post-stimulus potentials across an ensemble of trials (ensemble average). Averaging is presumed to decrease the size of the noise component, while leaving the signal component unchanged, thereby enhancing the signal-to-noise ratio. Since averaging is time-locked to a particular event onset, the result is called the average event-related potential (AERP). From this still widely accepted conceptualization (McGillem and Aunon, 1987), henceforth referred to as the signal-plus-noise (SPN) model, it follows that: (1) all the variability in single trial recordings is due to the independent ongoing noise component; (2) the AERP asymptotically approaches the true invariant evoked response as the number of trials involved in the averaging increases; and, most importantly, (3) when the AERP is subtracted from single trial recordings, the resulting residual time series do not contain significant event-related information. Rigorous acceptance of the SPN model assumptions would imply that no event-related modulation should be observed in statistical measures that are, by definition, computed on the residual time series. These measures include cross-correlation, spectral coherence and power spectrum density time functions. However, as pointed out above, there is abundant experimental evidence that event-related modulation does occur, suggesting that the SPN model is significantly violated in its main principles: (1) the ongoing activity can be event-related as a consequence of, for example, non-linear interactions between the evoked response and the ongoing activity, and (2) the evoked response may vary from trial to trial.

For the purpose of this work, we focus on the consequences of relaxing the SPN model's assumption of stationarity[1] of the evoked response over trials. The alternative model, henceforth referred to as the variable signal plus ongoing noise activity (VSPN) model, asserts that the stimulus-triggered response has a stereotyped waveform with variable amplitude and latency onset across trials. According to the VSPN model, after subtracting out the AERP, the single trial residual time series contain two components: (1) a stimulus phase-locked component resulting from the trial-to-trial amplitude and latency variability; and (2) an ongoing noise component.

Because the VSPN model includes a residual stimulus phase-locked component, it differs from the SPN model in its prediction concerning the post-stimulus modulation of power spectral density and statistical interdependence time functions. In the SPN model, the residuals remaining after AERP subtraction consist only of event-independent noise. Therefore, it predicts that the ensemble variance will be constant for all post-stimulus times. By contrast, the VSPN model predicts that the ensemble variance time function will of necessity be non-stationary, with its time course modulated according to the AERP waveform. Since the AERP is often oscillatory with clear characteristic frequencies, the phase-locked component remaining in the residuals will contribute to the power spectral density time function at these frequencies. Consequently, the power spectral density of the LFP or EEG time series, after subtraction of the AERP, and computed as a function of time in a sliding short window, can nonetheless be modulated according to the AERP waveform. Moreover, the ratio of the variance of

[1] Even though stationarity is usually assumed as a pre-condition, we argue that in practice it might be unattainable in most of the experimental designs involving behaving animals (see Section 4).

the residual stimulus phase-locked component to the variance of the ongoing component may change in time according to the AERP profile, especially if the time dependence of the variance of the ongoing component is weak. This means that if the residual time series from two recording channels co-vary, the time function of measures of those channels' statistical interdependence will also be modulated accordingly to the AERP profile. We refer to this type of modulatory effect on any such statistical measure as the *time-dependent signal-to-noise ratio effect*, where the signal refers again to remnants of the stimulus phase-locked components in the residual time series.

The existence of phase-locked components in the residual leads to a second contrast between the two models. Specifically, the VSPN model predicts that peaks in the single trial stimulus-locked component will be either larger or smaller than the average, resulting, after AERP subtraction, in the peaks of the phase-locked component in the single trial residual time series having either positive or negative polarity. If the latency variability is small, then the phases of the Fourier components at frequencies corresponding to the main characteristic frequencies of the AERP, are predicted to have a bimodal distribution. This again is in contrast with the SPN model, which predicts a flat phase distribution since the residuals are considered to originate only from the independent ongoing activity.

The VSPN model's predictions for these statistical measures are explicitly derived in Section 2.1. The predictions for the single channel quantities, variance and power time functions, and for the phase distribution are derived first. Then, the predictions for time functions of statistical interdependence measures (cross-correlation and coherence) are presented, and the time-dependent signal-to-noise ratio effect is illustrated using simulated time series. Section 3 presents the outcome of testing these predictions on LFP data recorded from implanted intra-cortical electrodes in monkeys performing a visual pattern discrimination task (Bressler et al., 1993). We emphasize that knowing the detailed characteristics of the interdependence measures under the influence of the remnant phase locked components is important since they provide a benchmark to discriminate whether a temporally modulated quantity in a given experiment is related to genuine event-related modulation of ongoing activity, or is due to the effect examined here.

Following the previous discussion, it thus becomes a fundamental task to reconstruct the single trial evoked response. If one is able to achieve that, then the ensemble average of the aforementioned statistical measures, when calculated on the new residual time series after removing the evoked response on a trial by trial basis, will exhibit no time behavior that is characteristically related to the trial-to-trial non-stationarity of the evoked response. Assuming the VSPN model, we apply a Bayesian inference procedure to estimate the single trial evoked responses in the LFP data set, which gives further and definitive support for the signal-to-noise ratio effect in the statistical quantities. The single trial based procedure again points to the importance of identifying the sources of non-stationary variance in LFP data. This is particularly imperative when considering the event-related modulation of statistical measures that is commonly interpreted as being due to fast changes in functional connectivity or other intrinsic neural parameters and opens the path for discovering temporal effects of neural dynamics that are caused by the underlying physiology. Additional progress in this direction will depend on the development of more accurate models of the single trial evoked response.

2. Methods

2.1. Model

The SPN model can be formally expressed as follows:

$$Z^r(t) = E(t) + \xi^r(t) \tag{2.1}$$

where $Z^r(t)$ is the recorded cortical LFP at time t for the rth trial, $E(t)$ is the stereotyped stimulus evoked response, and $\xi^r(t)$ is a zero-mean noise component, independent of the stimulus response, which represents ongoing noise activity. The stimulus onset is at $t = 0$. In practice, the average $\langle Z^r(t)\rangle$ taken over an ensemble of trials, $\{Z^1(t), Z^2(t), \ldots, Z^N(t)\}$, is considered to be a consistent estimate of $E(t)$, i.e. $E(t) = \langle Z^r(t)\rangle$, and the ongoing noise is estimated as the residual remaining when the average is subtracted from the LFP time series, i.e.

$$\eta^r(t) = Z^r(t) - \langle Z^r(t)\rangle = \xi^r(t). \tag{2.2}$$

A more generic alternative model, which takes into account the trial-to-trial variability of the evoked response, can be expressed by:

$$Z^r(t) = E^r(t) + \xi^r(t), \tag{2.3}$$

where $\xi^r(t)$ again represents the zero-mean ongoing noise activity. The evoked response $E^r(t)$ is now trial dependent, and could potentially have complex attributes, like the summation of distinct components, each one of them having their own trial-to-trial non-stationarity. In this work, we focus on the case where the evoked response has a stereotyped waveform with amplitude and latency variability, which is expressed as the VSPN model:

$$Z^r(t) = \alpha^r E(t + \tau^r) + \xi^r(t), \tag{2.4}$$

where the term α^r is a parameter corresponding to the amplitude of the evoked waveform and is assumed to be time independent for a given trial, and τ^r gives the single trial latency of the evoked response. The terms α^r, τ^r and ξ^r are assumed to be independent of each other.

2.1.1. The VSPN model and its predictions for the single channel quantities

The effects of trial-to-trial variability in amplitude and latency in the VSPN model are analyzed separately. Their role in determining the relation between the ensemble mean

and ensemble variance will be central to understanding the post-stimulus behavior of power and interdependence measures.

2.1.1.1. Amplitude variability.. Considering the amplitude variability alone, the VSPN model simplifies to:

$$Z^r(t) = \alpha^r E(t) + \xi^r(t). \tag{2.5}$$

The ensemble average (AERP) based on this model becomes $\langle Z^r(t)\rangle = \langle \alpha^r\rangle E(t)$. When the AERP is subtracted from a single trial, the residual time series becomes:

$$\begin{aligned}\eta^r(t) &= \alpha^r E(t) - \langle Z^r(t)\rangle + \xi^r(t) = (\alpha^r - \langle \alpha^r\rangle)E(t) + \xi^r(t)\\ &= S^r(t) + \xi^r(t),\end{aligned} \tag{2.6}$$

which contains two components: the ongoing activity $\xi^r(t)$ and a component that is dependent on the AERP waveform:

$$S^r(t) = (\alpha^r - \langle \alpha^r\rangle)E(t). \tag{2.7}$$

Thus, the VSPN model predicts that a stimulus phase-locked component will remain in the residual time series of LFP data after the AERP is subtracted from each trial.

The variance of $Z^r(t)$ over the ensemble of trials at a given time t is equal to the ensemble variance of the residual $\eta^r(t)$ which from Eq. (2.6) becomes:

$$\sigma^2(t) = \langle [\eta^r(t)]^2\rangle = \langle [S^r(t)]^2\rangle + \langle [\xi^r(t)]^2\rangle = \sigma_S^2(t) + \sigma_\xi^2(t), \tag{2.8}$$

where the variance of the stimulus phase-locked component is given by:

$$\sigma_S^2(t) = \langle [\alpha^r - \langle \alpha^r\rangle]^2\rangle E^2(t). \tag{2.9}$$

Since $\xi^r(t)$ is assumed to be stationary over the trial length, it follows that the variance of the residual has a time course resembling that of $E^2(t)$. In particular, the peaks of the variance function occur at the same times as the extrema of the AERP. Moreover, the power spectral density time function of the residual, $\langle |\eta^r(f,t)|^2\rangle$, computed in a sliding time window centered at time t, will also be modulated according to the AERP shape at frequencies characteristic of the AERP waveform. Specifically, since $E(t)$ is often oscillatory with a very distinct main frequency, the quantity $\langle |\eta^r(f,t)|^2\rangle$, at this frequency, will be similarly modulated and should also exhibit a significant increase during the evoked response time period.

Since the amplitude of the phase-locked component, α^r, can be either greater or less than the average on any single trial, it follows that $(\alpha^r - \langle \alpha^r\rangle)$ can take both positive and negative values. Therefore, the Fourier component at the characteristic frequency f, $\eta(f)$, exhibits a phase distribution having two modes that represent the positive and negative amplitudes, and thereby differ by the value of 180°. By contrast, if the phase-locked component in the residual were zero, as predicted by the SPN model, a uniform phase distribution would result.

2.1.1.2 Latency variability. When only the latency variability is considered, the VSPN model simplifies to:

$$Z^r(t) = E(t + \tau^r) + \xi^r(t). \tag{2.10}$$

To evaluate the effect of the right-hand side of Eq. (2.10), we use the Taylor expansion of $E(t + \tau^r)$ for small τ^r, which up to the first order is:

$$E(t + \tau^r) = E(t) + E'(t)\tau^r, \tag{2.11}$$

where $E'(t)$ is the first derivative with respect to t. The approximation to (2.10) then becomes:

$$Z^r(t) = E(t) + E'(t)\tau^r + \xi^r(t). \tag{2.12}$$

By letting $\langle \tau^r\rangle = 0$, the ensemble mean is then given by:

$$\langle Z^r(t)\rangle = \langle E(t)\rangle = E(t), \tag{2.13}$$

and the residual time series becomes:

$$\begin{aligned}\eta^r(t) &= E(t) - \langle Z^r(t)\rangle + E'(t)\tau^r + \xi^r(t) = E'(t)\tau^r + \xi^r(t)\\ &= S^r(t) + \xi^r(t).\end{aligned} \tag{2.14}$$

Again the residual time series contain a component, $S^r(t) = E'(t)\tau^r$, that is phase-locked to stimulus onset. From Eq. (2.14) we obtain the ensemble variance as

$$\begin{aligned}\sigma^2(t) &= \langle [\eta^r(t)]^2\rangle = \langle [\tau^r]^2\rangle [E'(t)]^2 + \langle [\xi^r(t)]^2\rangle\\ &= \sigma_S^2(t) + \sigma_\xi^2(t),\end{aligned} \tag{2.15}$$

where the variance of the phase-locked component is approximately:

$$\sigma_S^2(t) = \langle [\tau^r]^2\rangle [E'(t)]^2. \tag{2.16}$$

This equation shows that the ensemble variance is again modulated by the evoked response since it follows the square of the first derivative of the evoked response. Eq. (2.16) allows us to predict the form of the variance function when the AERP resembles a damped sinusoid. That is because the derivative of a sinusoid has the property of being shifted by 90°. Specifically, maximum values in variance should coincide in time with inflexion points of the AERP, and minimum values in variance with extrema of the AERP.

2.1.1.3. Amplitude and latency variability. When both amplitude and latency vary from trial to trial, their interplay can have more complicated effects. We use a simple example to illustrate the effect of increasing latency variability while maintaining a constant level of amplitude variability (Fig. 1). The simulated time series are given by $Z^r(t) = \alpha^r E(t + \tau^r)$, without added noise, and with the waveform given by $E(t + \tau^r) = H(t + \tau^r)sin(\omega t + \phi^r)$. The phase of the sine function is given by $\phi^r = \tau^r\omega$ and $H(t)$ is a Hanning window, used to produce a waveform that mimics commonly observed AERPs. The signal $E(t)$ contains two full cycles of a sinusoidal oscillation with

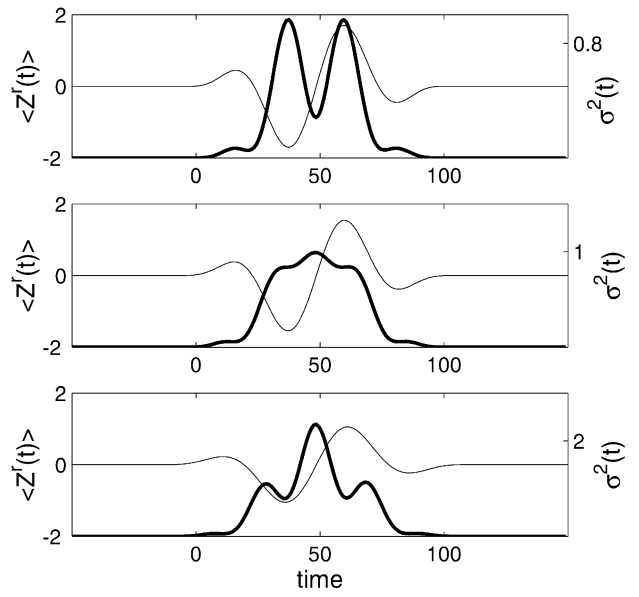

Fig. 1. Relation between ensemble average, $\langle Z^r(t)\rangle$, and ensemble variance time function, $\sigma^2(t)$, for the case of trial-to-trial amplitude and latency variability in simulated time series. The simulated evoked signal $E(t)$, consisted of two full cycles of a sinusoidal waveform (see text). The waveform is shown by the thin curve while the ensemble variance time function is shown by the thicker curve. Single trial amplitudes were taken from a uniform distribution over the interval [0,4]. The latency parameter expressed in terms of phase was uniformly distributed over the following intervals: $[-\pi 10, \pi/10]$ (top plot), $[-\pi/4, \pi/4]$ (middle plot) and $[-\pi/2, \pi/2]$ (bottom plot). When the amplitude variability dominates (top plot), the ensemble variance peaks coincide with extrema of the AERP. As the latency variability increases, amplitude and latency are balanced, resulting in a single peak being observed (middle plot). As latency variability increases even further, the variance peaks coincide with inflexion points of the AERP waveform, and variance valleys coincide with extrema of the AERP (bottom plot). A total of 2000 trials were employed. Amplitude, variances and time are given in arbitrary units.

period $T = 50$ (arbitrary time unit), and is zero elsewhere. The amplitudes α^r were taken from a uniform distribution over the interval [0,4]. The latency parameter expressed in terms of phase was uniformly distributed over the following intervals: $[-\pi/10, \pi/10]$ (top plot), $[-\pi/4, \pi/4]$ (middle plot) and $[-\pi/2, \pi/2]$ (bottom plot).

For small latency variability, the amplitude variability modulation on the ensemble variance dominates, resulting in variance peaks that coincide with extrema of the AERP (top plot), in accordance with the derived Eq. (2.9). As the latency variability increases, a point is reached where amplitude and latency effects are balanced, leading to a single peak in the variance function (middle plot). As latency increases even further (bottom plot), the characteristic effect of latency variability, as described by the linear approximation in Eq. (2.16), emerges. As can be seen, this approximation holds well even for latencies uniformly distributed over an interval ranging about half of the waveform's cycle. At much higher levels of latency variability (not shown), a single peaked variance is observed.

2.1.2. Implications of the VSPN model for statistical interdependence measures involving two channels

Consider two channel recordings given by $Z_1^r(t) = \alpha_1^r E_1(t) + \xi_1^r(t)$ and $Z_2^r(t) = \alpha_2^r E_2(t) + \xi_2^r(t)$. The cross-correlation function between the two channels' time series, at time t and time lag τ is then given by:

$$C_{Z_1Z_2}(\tau,t) = \frac{\langle S_1^r(t)S_2^r(t+\tau)\rangle + \langle \xi_1^r(t)\xi_2^r(t+\tau)\rangle}{\sqrt{\langle [S_1^r(t)]^2\rangle + \langle [\xi_1^r(t)]^2\rangle}\sqrt{\langle [S_2^r(t+\tau)]^2\rangle + \langle [\xi_2^r(t+\tau)]^2\rangle}}, \quad (2.17)$$

where $S_1^r(t) = (\alpha_1^r - \langle \alpha_1^r\rangle)E_1(t)$ and $S_2^r(t) = (\alpha_2^r - \langle \alpha_2^r\rangle)E_2(t)$. Without loss of generality, we assume that the ongoing noise processes are approximately stationary, meaning that $\langle \xi_1^r(t)\xi_2^r(t+\tau)\rangle$, $\langle [\xi_1^r(t)]^2\rangle$ and $\langle [\xi_2^r(t+\tau)]^2\rangle$ have no time dependence. That is, the cross-correlation function between the noise processes, $\xi_1^r(t)$ and $\xi_2^r(t+\tau)$, is only a function of the time lag τ and is time independent: $C_{\xi_1\xi_2}(\tau,t) = C_{\xi_1\xi_2}(\tau) = \langle \xi_1^r(t)\xi_2^r(t+\tau)\rangle / \sqrt{\langle [\xi_1^r(t)]^2\rangle \langle [\xi_2^r(t+\tau)]^2\rangle}$. The cross-correlation function between the two evoked signals, considering the case of trial-to-trial amplitude variability, is given by:

$$C_{S_1S_2}(\tau,t) = \frac{\langle (\alpha_1^r - \langle \alpha_1^r\rangle)(\alpha_2^r - \langle \alpha_2^r\rangle)\rangle E_1(t)E_2(t+\tau)}{\sqrt{\langle [\alpha_1^r - \langle \alpha_1^r\rangle]^2\rangle}\sqrt{\langle [\alpha_2^r - \langle \alpha_2^r\rangle]^2\rangle}|E_1(t)||E_2(t+\tau)|} = \pm K, \quad (2.18)$$

for $E_1(t) \neq 0$, $E_2(t+\tau) \neq 0$ and where K is the correlation coefficient of the two single-trial amplitudes. Although $|C_{S_1S_2}(\tau,t)|$ is a constant, $C_{S_1S_2}(\tau,t)$ may flip between positive and negative values of K, depending on the sign of the product $E_1(t)E_2(t+\tau)$, which may change in time for a given time lag. Thus, the very presence of the variable signals in the VSPN model already makes possible temporal modulations of the cross-correlation function between the two time series, $C_{Z_1Z_2}(\tau,t)$, albeit in a simple and very stereotypical way. The interplay between signals and noises can lead to more complex and significant temporal modulations of $C_{Z_1Z_2}(\tau,t)$, as we consider below.

Let *SNR* represent the signal-to-noise ratio, defined as $SNR_1(t) = \sigma^2_{S_1}(t)/\sigma^2_{\xi_1}(t)$ and $SNR_2(t+\tau) = \sigma_{S_2}{}^2(t+\tau)/\sigma_{\xi_2}{}^2(t+\tau)$. Dividing both the numerator and denominator by $\sigma_{\xi_1}(t)\sigma_{\xi_2}(t+\tau)$, and after algebraic manipulation, Eq. (2.17) can be rewritten as:

$$C_{Z_1Z_2}(\tau,t) = \frac{\sqrt{SNR_1(t)SNR_2(t+\tau)}C_{S_1S_2}(\tau,t) + C_{\xi_1\xi_2}(\tau)}{\sqrt{SNR_1(t)+1}\sqrt{SNR_2(t+\tau)+1}} \quad (2.19)$$

It is clear that complex temporal modulation can result depending on the time course of the signal-to-noise ratios. In particular, as the product of the signal-to-noise ratios, $SNR_1(t)SNR_2(t+\tau)$, increases, the cross-correlation function approaches the evoked signals' cross-correlation function, i.e. $C_{Z_1Z_2}(\tau,t) \to C_{S_1S_2}(\tau,t)$. As seen in the previous section, fluctuations in the signal-to-noise ratios are expected to occur since the variances in signals have their time course modulated by the square of the AERP waveform. Two characteristic cases illustrating this effect, referred to as the *time-dependent signal-to-noise ratio effect*, are discussed below.

Case 1. Transient increase in cross-correlation. To illustrate this effect, consider the situation where for a given time

lag τ, we have that $C_{S_1S_2}(\tau,t) = K > C_{\xi_1\xi_2}(\tau)$ and that $SNR_1(t) \approx SNR_2(t+\tau)$. Thus the stimulus phase-locked components in the residual time series co-vary at a level greater than that of the ongoing noise and the two AERPs have similar waveforms but are separated by a time difference of τ. Eq. (2.19) then becomes:

$$C_{Z_1Z_2}(\tau,t) = \frac{SNR_1(t)K + C_{\xi_1\xi_2}(\tau)}{SNR_1(t)+1}. \quad (2.20)$$

This function is a monotonically increasing function of $SNR_1(t)$, and if we assume that $\sigma^2_{\xi_1}(t)$ is constant, $C_{Z_1Z_2}(\tau,t)$ will follow the profile of $\sigma^2_{S_1}(t)$. Therefore, peaks of the cross-correlation function will coincide with peaks in the variance of the stimulus phase-locked component, and hence, as demonstrated above, with extrema of the AERP. This predicted signature will be demonstrated in the analysis of LFP data that follows, suggesting that this case represents a realistic situation. The possibility will be discussed that cross-correlation increases, due to signal-to-noise ratio variation, might be misconstrued as reflecting modulation in the level of synchronization between two neuronal populations.

An example of this effect is now provided (Fig. 2, left

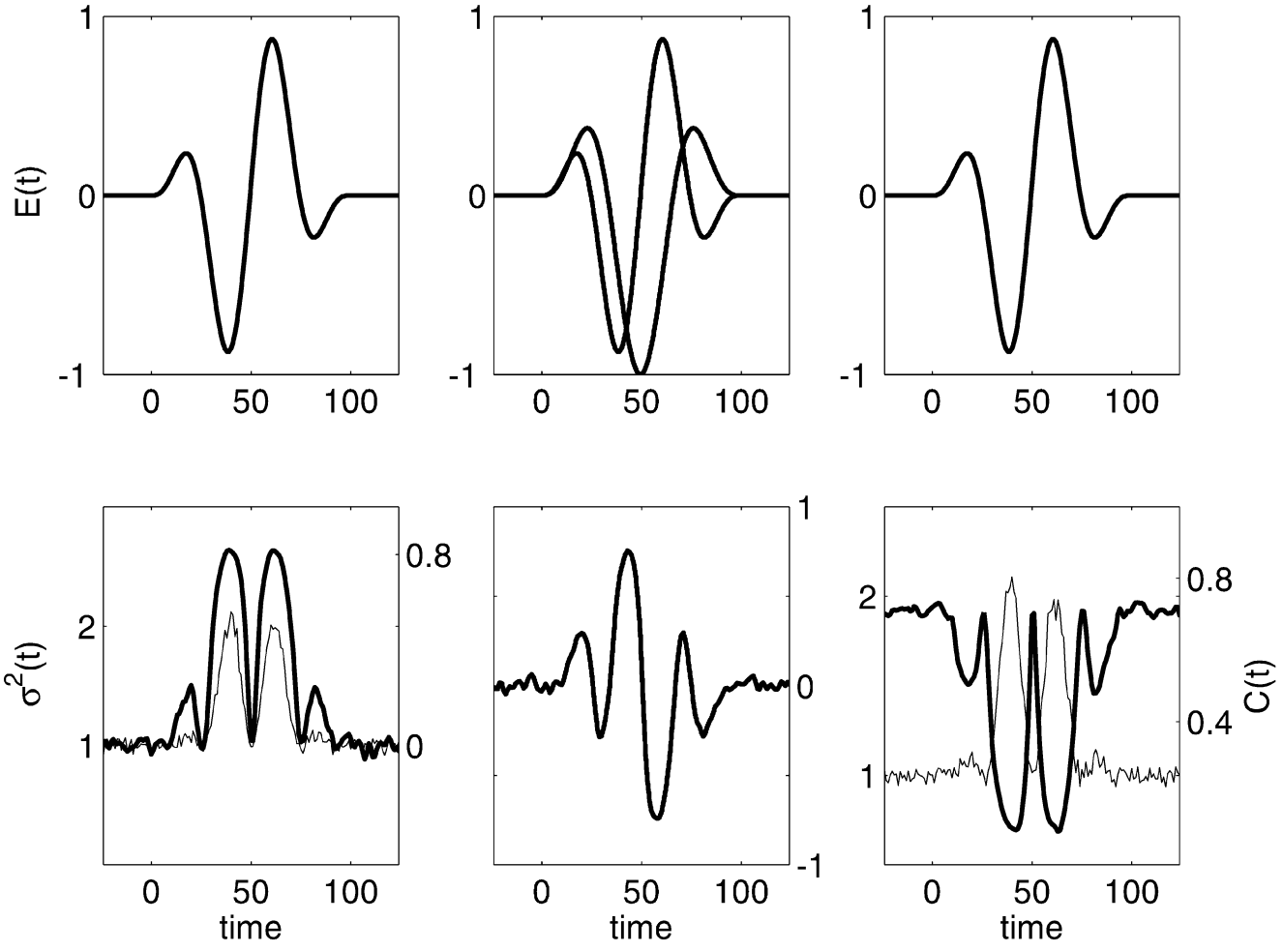

Fig. 2. Time-dependent signal-to-noise ratio effect on the modulation of the cross-correlation time function. Transient increase I (left column). The two channels share a common evoked response $E(t)$ (top plot) whose amplitude is drawn from a uniform distribution over the interval [0,4]. Each channel's ongoing activity was modeled as independent zero mean and unit variance white Gaussian noise (see text). In the bottom plot, the zero lag cross-correlation $C(t)$ (thick curve) and the ensemble variance $\sigma^2(t)$ time functions are shown ($\sigma^2(t)$: left vertical axis; $C(t)$: right vertical axis). The variance (and the signal-to-noise ratio) of the shared evoked component oscillates at 1/2 the period of the original sinusoidal component. As a consequence, the cross-correlation time function also oscillates with the same period, with peaks coinciding in time with peaks in the variance, or equivalently, with extrema of the evoked response. Transient increase II (middle column). Top: simulated evoked responses, $E(t)$, from two channels. Parameters for the evoked response-waveforms, amplitudes and ongoing noise are the same as in the previous example, except that the periods of the two evoked signals are slightly different. Bottom: only the zero-lag cross-correlation is shown. The peaks, i.e. extrema, in the cross-correlation function in general may not coincide in time with extrema of $E(t)$ or equivalently with peaks of the ensemble variance from each channel. Notice also the fluctuations of the cross-correlation between positive and negative values. Transient decrease (right column). Top: the same parameters as before except that the trial-to-trial amplitudes for the common evoked responses for each channel are independent, while the ongoing noise is now correlated. Bottom: the signal-to-noise ratio effect appears as a transient decrease in cross-correlation that could resemble a transient desynchronization event. Peaks in the variance time function of the time series from each channel coincide with minima of the cross-correlation time function. In all simulations, the ensemble consisted of 2000 trials. Amp1itude, variances and time are given in arbitrary units. The ensemble variance time functions of each channel are approximately the same and only one of them is shown in the right and left bottom plots.

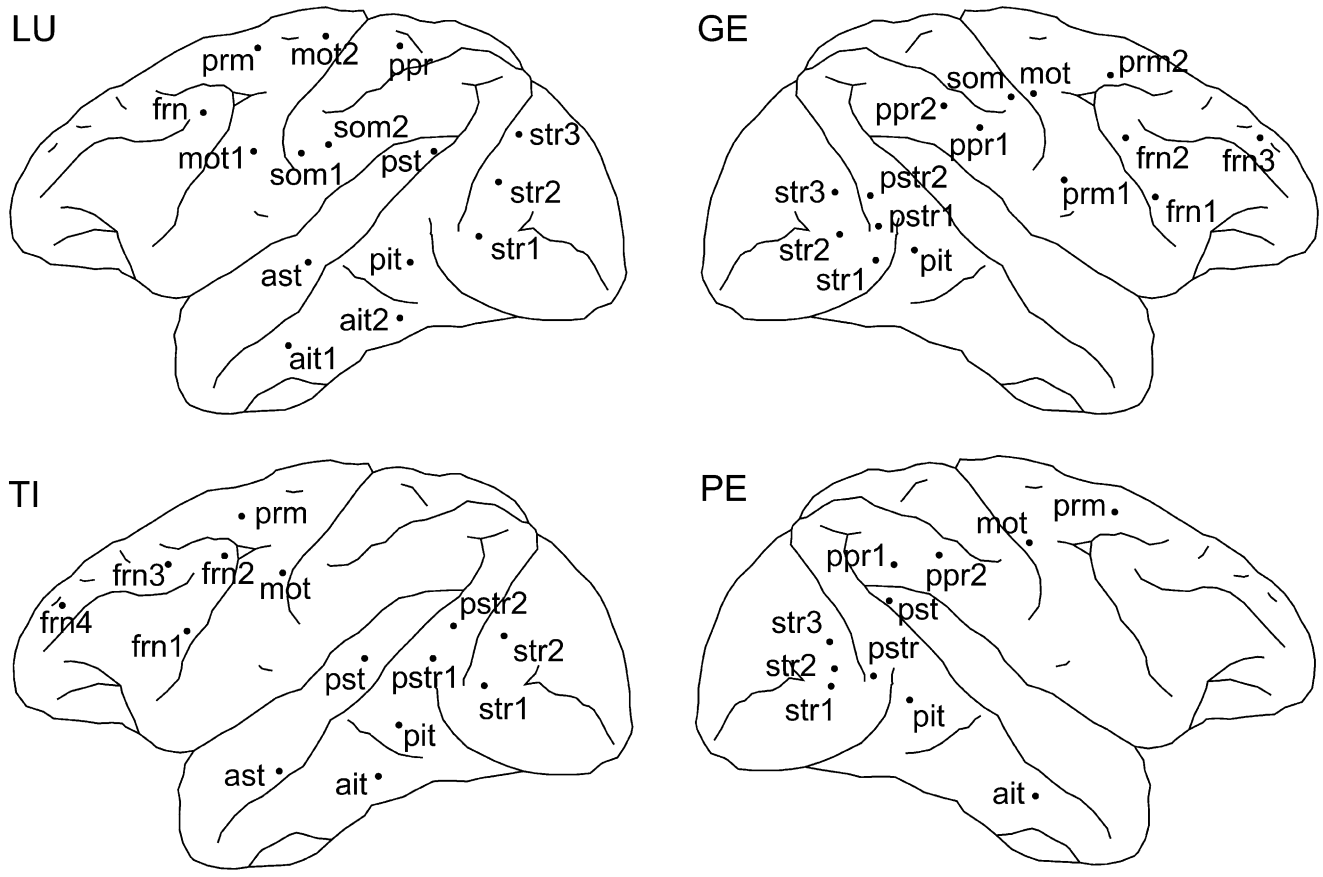

Fig. 3. Sites for the transcortical electrodes placement. Labels: striate (str); pre-striate (pstr); posterior inferior temporal (pit); anterior inferior temporal (ait); posterior superior temporal (pst); anterior superior temporal (ast); posterior parietal (ppr); somatosensory (som); motor (mot); pre-motor (prm); frontal (frn). Recordings in LU and TI are from the left hemisphere.

column), with two simulated time series described as: $Z_1^r(t) = \alpha^r E(t) + \xi_1^r(t)$ and $Z_2^r(t) = \alpha^r E(t) + \xi_2^r(t)$. The time series share a common signal that is given by $E(t) = H(t)\sin(\omega t)$, consisting of two cycles (period $T = 50$), existing from $t = 0$ to $t = 100$, and zero elsewhere. $H(t)$ is a Hanning window. The ongoing activities are simply modeled as zero-mean, unit-variance, Gaussian, white-noise processes. The single trial amplitudes α^r are the same for the two channels and are drawn from a uniform distribution over the interval [0,4]. The zero-time-lag, point-by-point cross-correlation is computed according to Eq. (2.23). As expected, it peaks at the same times as the variance of the residuals (i.e. at the signal-to-noise ratio peaks) and oscillates at half the period of $E(t)$.

For situations where the main characteristic frequencies of $E_1(t)$ and $E_2(t)$ are significantly different, peaks in the cross-correlation function may no longer coincide precisely with peaks in variance, although as before, the same time-dependent signal-to-noise ratio effect will be observed, i.e. $C_{Z_1Z_2}(\tau,t) \rightarrow C_{S_1S_2}(\tau,t)$ as the signal-to-noise ratio increases (Fig. 2, middle column).

Case 2. Transient decrease in cross-correlation. We next consider the situation where the stimulus phase-locked components $S_1^r(t)$ and $S_2^r(t+\tau)$ in the residual time series do not co-vary, i.e. $\langle(\alpha_1^r - \langle\alpha_1^r\rangle)(\alpha_2^r - \langle\alpha_2^r\rangle)\rangle = 0$, but the ongoing activities are correlated, for example, $\langle\xi_1^r(t)\xi_2^r(t+\tau)\rangle = C_{\xi_1\xi_2}(\tau) > 0$. Assuming as before that the time dependence of $\sigma^2_{\xi_1}(t)$ and $\sigma^2_{\xi_2}(t+\tau)$ are weak, then the value of the observed cross-correlation $C_{Z_1Z_2}(\tau,t)$ will still be modulated by the time dependence of the product of the signal-to-noise ratios. As the signal-to-noise ratio product increases, the observed cross-correlation time function approaches that of the stimulus phase-locked components, which is zero. In practice, the resulting modulation could be misconstrued as a short transient desynchronization episode between two recorded neuronal populations (see Fig. 2, right column).

For frequencies f related to the main oscillatory components of the evoked signals, the same effects described in cases 1 and 2 will also be observed in the time-varying spectral coherence function:

$$G_{Z_1Z_2}(f,t) = \frac{|\langle S_1^r(f,t)S_2^{r*}(f,t)\rangle + \langle\xi_1^r(f,t)\xi_2^{r*}(f,t)\rangle|}{\sqrt{\langle|S_1^r(f,t)|^2\rangle + \langle|\xi_1^r(f,t)|^2\rangle}\sqrt{\langle|S_2^r(f,t)|^2\rangle + \langle|\xi_2^r(f,t)|^2\rangle}}, \quad (2.21)$$

which is computed in a sliding time window centered at time t. This can be easily verified considering the similarity between Eqs. (2.21) and (2.17).

Even though we have only considered fluctuations in signal-to-noise ratio that originate from trial-to-trial amplitude variability of the evoked signals, latency variability will result in similar fluctuations, and consequently in temporal modulation of the same interdependence measures. For latency variability that is not too large, peaks in the signal-to-noise ratios are expected to coincide with inflexion points of the AERP waveform, rather than with extrema as in the case of amplitude variability just described. For the more realistic case where both amplitude and latency variability occur, the combined effect will depend on which one dominates the modulation of ensemble variance, as exemplified in Fig. 1.

2.2. Experiments and data analysis

2.2.1. Behavioral task

Experiments were performed on four macaque monkeys (LU, GE, PE and TI) in the Laboratory of Neuropsychology at the National Institute of Mental Health. Animal care was in accordance with institutional guidelines at the time. A detailed description of the experiment has previously been presented (Bressler et al., 1993). The monkeys performed a visual pattern discrimination task in which they sat facing a visual display screen. Each trial began with self-initiated depression of a hand lever with the preferred hand. Following a random interval from 0.5 to 1.2 s, a visual stimulus appeared on the screen for 100 ms. The stimulus was one of two pattern types: four dots arranged as a diamond or as a line. The monkey indicated its discrimination of line and diamond patterns by releasing (GO) or maintaining (NO-GO) pressure on the lever. The monkey received a water reward for correct GO performance. GO and NO-GO trials were randomly presented with equal probability in 1000-trial sessions. The contingency between stimulus pattern and response type was reversed across sessions. The present study focuses on the initial stages of the visual evoked response to presentation of the line pattern type. For each ensemble, the following number of trials were used: 2344, 888, 914 and 2053 for the monkeys LU, GE, PE and TI, respectively. For each monkey, the ensemble of trials was balanced for response type (GO and NO-GO).

2.2.2. Recording and data preprocessing

LFPs were sampled at 200 Hz from chronically implanted surface-to-depth transcortical bipolar electrodes at 11 to 15 cortical sites in the cerebral hemisphere contralateral to the preferred hand. Approximate localization of the electrodes in each monkey are shown in Fig. 3. Each trial was recorded from approximately 115 ms pre-stimulus onset to 500 ms post-stimulus. The LFPs in each trial were linearly detrended, 60 Hz removed, and normalized to zero mean and unit variance (time normalization). After these preprocessing steps, the AERPs (ensemble averages) and ensemble variance time functions were computed, and constitute then normalized quantities. In addition, each ensemble of trials was normalized at each time point to zero ensemble mean and unit ensemble variance (ensemble normalization). The resulting residual time series were employed in the computation of the phase histograms, cross-correlations and spectral quantities described below.

2.2.3. AMVAR spectral estimation

Power and coherence time functions were estimated by the application of adaptive multivariate autoregressive (AMVAR) models to the residual time series (Ding et al., 2000). Each single trial residual (600 ms long) was divided into 110 consecutive and overlapping (shifted by one data point) windows of 10 points (50 ms) each. An MVAR model of order 5 was adaptively computed for each successive window using the LWR algorithm (Haykin and Kesler, 1983). A spectral matrix was derived for each time window from the model coefficients, and then used as the basis for computing power and coherence spectra in the range of 0–100 Hz. The squared coherence values were used. The moving time windows then allowed the construction of power and coherence time functions for any frequency bin. AMVAR spectral estimation was employed instead of the traditional non-parametric approach of directly applying the direct Fourier transform (DFT) to the time series data because the DFT is an extremely biased estimate when used in such short time windows. The choice of 50 ms as the time window duration came from previous experience with the application of AMVAR analysis to this data set (Ding et al., 2000). Overall, the use of short time windows in this paper was motivated by the need for tracking non-stationary transient cortical processes on a sub-second time scale. Particular attention was given to power and coherence at the 12 Hz spectral component. This had two main motivations. Following the VSPN hypothesis, the stimulus phase-locked component in the residual should have the same frequency content as that of the AERP. For many of the channels having a significant evoked response, the early post-stimulus portion of the AERP was found to have a clear characteristic oscillation with a period around 80 ms (12.5 Hz). In agreement, previous results on this data set (Bressler et al., 1999) highlighted the existence of peaks near 12 Hz in power and coherence spectra for many cortical sites, specially during the early stages of the evoked response (up to approximately 200 ms after stimulus onset).

2.2.4. Absolute phase histograms

In order to compare predictions of the SPN and VSPN models regarding the distribution of phase, spectral phase estimates from Fourier transformed single trial residual time series were computed. In AMVAR spectral estimation, absolute phase information for single trials is lost and cannot be recovered. Alternative methods for calculating the instantaneous phase, such as the Hilbert transform and complex demodulation, were considered inadequate mainly because they would require narrow band-pass filtering of the data, and consequently high order filters and very long time

segments of data. We approached the phase estimation problem in terms of optimal fitting in the least square sense. It is known that the Fourier transform of a time series at a specific frequency represents an optimal fit of the time series by sine and cosine functions at that frequency (Chatfield, 1995). For this reason, the FFT was used to obtain single trial phase estimates for constructing the phase distribution. The choice of window length for the FFT was constrained by three factors: (a) the use of short windows to track the time evolution of the phase distributions from pre-stimulus to post-stimulus periods; (b) the FFT constraint on the window length being a power of 2 (the alternative of zero padding introduces artifacts in the computation of phase distributions); and (c) the choice of the 12 Hz Fourier component as an indicator of the main characteristic frequency of the AERPs (see Section 2.2.3 above). These constraints resulted in the following procedure. FFTs were performed on a time window (80 ms long) moving one data point at a time, from 50 ms before the stimulus onset to 350 ms after. The phase estimates of the 12 Hz (12.5 Hz being the actual frequency since we are using a 80 ms window) components for a window starting at time t, from the whole ensemble of single trials, were then collected to build the phase histogram at time t for a specific channel and subject. Each histogram's bin width was set to $\pi/50$ rad.

2.2.5. Testing for departure from uniform phase distribution

The SPN model predicts a uniform phase distribution. To assess whether a given absolute phase distribution departed from the uniform distribution, the modified Kuiper test (Fisher, 1995) for circular data was employed. In this procedure, for a specific time window and for an ensemble of N trials, the linear order statistics $x^r = \phi^r/2\pi, \ldots, x^r = \phi^r/2\pi$ were first calculated, where ϕ^r was the phase of the 12 Hz Fourier component for trial r. Second, we obtained from the ensemble of N trials, the statistics:

$$D_N^+ = \max\left(\frac{1}{N} - x^1, \frac{2}{N} - x^2, \ldots, 1 - x^N\right) \tag{2.22}$$

$$D_N^- = \max\left(x^1, x^2 - \frac{1}{N}, x^3 - \frac{2}{N}, \ldots, x^N - \frac{N-1}{N}\right)$$

$$V_N = D_N^+ + D_N^-$$

Third, we computed the final statistic $V = V_N(N^{1/2} + 0.155 + 0.24/N^{1/2})$. V was compared to critical values (V_c) given by the Kuiper modified statistics. At the significance level of $P < 0.01$, $V_c(0.01) = 2.0$. Since the phase distributions were computed as functions of time with the sliding window approach, the Kuiper V was also calculated as a time function for each channel from each monkey.

2.2.6. Cross-correlation time function

The cross-correlation at time t between the residual time series from a channel pair Z_1 and Z_2 was computed using

$$C_{Z_1Z_2}(\tau, t) = \frac{\sum_{r=1}^{N} [Z_1^r(t) - \langle Z_1^r(t)\rangle][Z_2^r(t+\tau) - \langle Z_2^r(t+\tau)\rangle]}{\sqrt{\sum_{r=1}^{N} [Z_1^r(t) - \langle Z_1^r(t)\rangle]^2 \sum_{r=1}^{N} [Z_2^r(t+\tau) - \langle Z_2^r(t+\tau)\rangle]^2}}, \tag{2.23}$$

where τ is the time lag and $\langle Z_1^r(t)\rangle$ denotes the trial ensemble average at time t. The cross-correlation was smoothed by computing it on the low-pass filtered (-3 db at 22 Hz) and pre-processed residual time series. Zero-phase forward and reverse digital filtering was employed to prevent phase distortion (FIR2 and FILTFILT functions from MATLAB, version 6, Natick, MA).

2.2.7. Estimation of single trial evoked responses

The VSPN model asserts that the trial-to-trial variability of evoked responses is responsible for temporal modulation of interdependence measures. This implies that if one is able to estimate the evoked response on a single trial basis and then separate it from the ongoing activity, interdependence measures computed on the new residual time series will not exhibit any characteristic time dependence. To examine this prediction, estimators for the single trial parameters were derived based on a Bayesian approach (Appendix A). Eq. (2.5) is written in terms of discrete times, $Z^r(k) = \alpha^r E(k + \tau^r) + \xi^r(k)$, and the latencies and amplitudes are estimated following the three steps below:

1. To make the solution unique, the norm of the evoked response $E(k)$ is constrained to equal 1. Let $k_a \le k \le k_b$ be a post-stimulus time segment where $E(k)$ is non-zero. Here k_a and k_b are indices for the first and last data point of the segment. The cross-correlation between the specified segment of the estimated evoked response and a correspondent segment of single trial data, i.e.

$$\frac{\langle E(k)Z^r(k+\tau)\rangle_k}{\sqrt{\langle E^2(k)\rangle_k \langle [Z^r(k+\tau)]^2\rangle_k}},$$

   for the specific rth trial, is then computed for different integer lags τ, with $k_0 + \tau > 0$ for k_0 corresponding to the sample at stimulus onset.
2. The lag that gives the maximum positive cross-correlation value is then chosen to represent the latency τ^r for the rth trial.
3. The estimated latency shift is introduced in the evoked response model and the amplitudes are then computed as: $\alpha^r = \langle Z^r(k)E(k+\tau^r)\rangle_k$. The values of $E(k+\tau^r)$ for times $k + \tau^r$ that fall outside of the sampled time series are set to zero.

The above algorithm was applied to the pre-processed macaque LFP recordings. After the single trial amplitudes and latencies were estimated, we subtracted the estimated evoked responses from the corresponding single trial data. Ensemble variance and coherence time functions were computed on the new residual time series, after the corre-

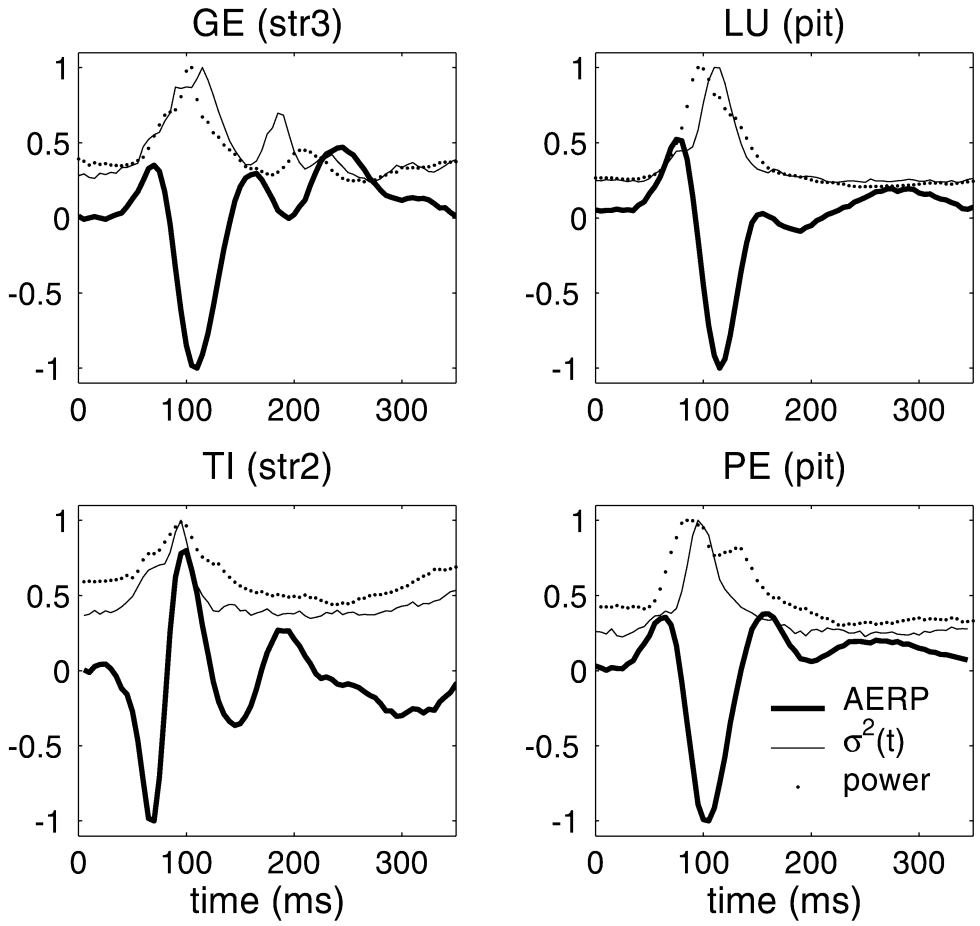

Fig. 4. Example time functions of ensemble mean (AERP), ensemble variance ($\sigma^2(t)$) and power density at 12 Hz. Variance and power are computed from the residual time series. To facilitate the comparison between the shapes, all quantities were normalized by their own maximal amplitude. Stimulus onset is at time 0 ms.

sponding time and ensemble normalization described in Section 2.2.2.

3. Results

3.1. Single channel quantities: AERP, variance and power

Predictions of the VSPN model were tested using the macaque LFP data. Fig. 4 shows example time functions of AERP, the ensemble variance and power density at 12 Hz (see Section 2 for the choice of this specific frequency) from selected channels for each of the four monkeys. The AERP functions often exhibited several extrema. The variance function followed the expected temporal profile from the VSPN model with amplitude variability as the main contributor: the peak times roughly coincided with the first two extrema times of the AERP. The power at 12 Hz computed from the AMVAR model also followed the same predicted time course but in most cases with less temporal resolution, since its computation required a time window of 50 ms duration, which smeared the temporal structure.

We note that not every channel showed clear AERPs and peaks in the variance functions. For those channels that exhibited clear peaks, we examined the predicted correspondence between the time of the largest variance peak and the time of the largest AERP extremum. The scatter plot in Fig. 5 combines the data from 30 channels from the four monkeys. The plot displays a general monotonic relation with points clustering around a line having slope of 0.74 (the VSPN model predicts a slope close to 1 for the case where the trial-to-trial amplitude variability is the dominant factor). The computed correlation coefficient was $R = 0.87$ ($R^2 = 0.76$). The same analysis for each individual monkey yielded the following results: GE, $R = 0.94$, including 6 channels in the striate, pre-striate, and parietal cortices; LU, $R = 0.72$, including 8 channels in the striate, pre-striate, inferior temporal, and superior temporal cortices; TI, $R = 0.89$, 9 channels in the striate, pre-striate, temporal, and frontal cortices; and PE, $R = 0.97$, 7 channels in the striate, pre-striate, inferior temporal and pre-motor.

3.1.1. Bimodal phase distributions

When amplitude variability is the main factor in the trial-to-trial variability of the evoked response, the VSPN model

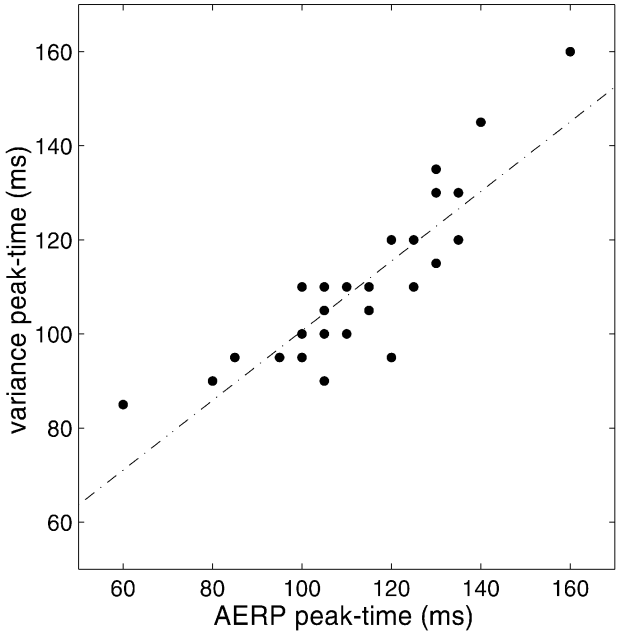

Fig. 5. Time of the largest peak in the variance function plotted against the time of the largest AERP extremum. Results from 30 channels from the 4 monkeys are shown. The dashed line is the least square linear fit (slope equal to 0.74) relating the peak-times of the AERP and variance time function. The VSPN model predicts a slope close to 1 for the case where the amplitude is the main source of trial-to-trial variability.

predicts a bimodal phase distribution for the residuals. This was tested by computing phase distributions of the 12 Hz component over the length of the trial (see Section 2.2.5). The Kuiper V statistic was computed for each phase distribution. Phase distributions having a Kuiper V value greater than $V_c = 2.0$ were judged to be significantly different ($P < 0.01$) from the uniform distribution.

Fig. 6 shows time functions of the Kuiper V statistic for selected channels from each monkey. As predicted by the VSPN model, the departure from uniform phase distribution is only observed following stimulus onset, during the stimulus evoked response. We found that all channels for all 4 monkeys had uniform phase distributions in the pre-stimulus period. By contrast, most channels in each monkey showed departure from the uniform distribution during stimulus processing period (0–200 ms), with exceptions being: GE (pstr2, som, frn2), LU (ppr, som1, mot2), TI (pst) and PE (pst, ppr1, ppr2, prm2). Notice that the maximum of the Kuiper V function tends to occur near 100 ms, which is about the time when maximal variance is observed (Fig. 6).

Since the Kuiper statistic only tells whether or not a distribution is uniform, the phase distributions that significantly departed from uniformity were visually inspected to further determine whether or not they were bimodal. Fig. 7 shows a representative phase distribution from each monkey, demonstrating clear-cut bimodality. For all the channels where we observed departure from the uniform distribution, the phase distributions were ascertained to have bimodality.

3.2. Cross-correlation and spectral coherence

Cross-correlation time functions were observed to be modulated by the signal-to-noise ratio at a variety of cortical sites, including striate, pre-striate, inferior temporal, parietal, motor and pre-frontal. Examples are shown in Fig. 8. The oscillatory nature of the cross-correlation time function predicted by the VSPN model, and the temporal relation of its peaks with peaks in variance, are evident. The period of the oscillations in the cross-correlation functions agrees roughly with that in the variance functions, and is half the period of the main AERP oscillatory component, as expected from the VSPN model.

To estimate the prevalence of this effect, we needed to examine the time relation between the time peaks in variance and cross-correlation for the whole data set. A problem that complicated this analysis was that the AERPs and variance functions from different channels often did not peak at the same time. This discrepancy was perhaps due to temporal delays in direct or indirect transmission between the channel pair, or to the difference in the arrival times of a common input signal to both channels. To circumvent this difficulty, we chose the time lag τ in the cross-correlation function as the separation time between the largest variance peaks from each channel in the concerned pair. When the main characteristic frequency of the AERPs from two channels are similar and amplitude variation is the main factor for the temporal modulation of variance, then the VSPN model predicts that the time of the largest peak in the cross-correlation function, lagged by τ, should coincide roughly with the time of the earliest large variance peak of the two channels. This prediction was tested in a total of 144 channel pairs from the 4 monkeys, selected according to the following criteria: (1) existence of clear peaks in the AERPs and variance functions; (2) the existence of non-uniform phase distributions events during the evoked response period; and (3) exceeding a conservative cross-correlation threshold ($|\text{cross-correlation extrema}| \geq 0.2$). Fig. 9 shows the relation between cross-correlation and first variance peak times. Superimposed is the line (slope ~0.94) obtained from the least square linear fit for the relation between peak-times in variance and cross-correlation. The VSPN model predicts a slope close to 1 for the case where the trial-to-trial variability in amplitude is the main contributor to fluctuations in signal-to-noise ratio. The correlation coefficient for the data in Fig. 9 is $R = 0.87$ ($R^2 = 0.76$), supporting the role of the time-dependent signal-to-noise effect on the temporal modulation of the cross-correlation function. The coefficients computed individually for each monkey were: LU, 44 channel pairs, $R = 0.90$; GE, 41 pairs, $R = 0.92$; TI, 43 pairs, $R = 0.86$; PE, 16 pairs, $R = 0.94$.

Similar time-dependent signal-to-noise ratio effects were also observed for coherence time functions. Two important characteristics were detected. First, a commonly observed effect was the existence of peaks around 12 Hz in the coher-

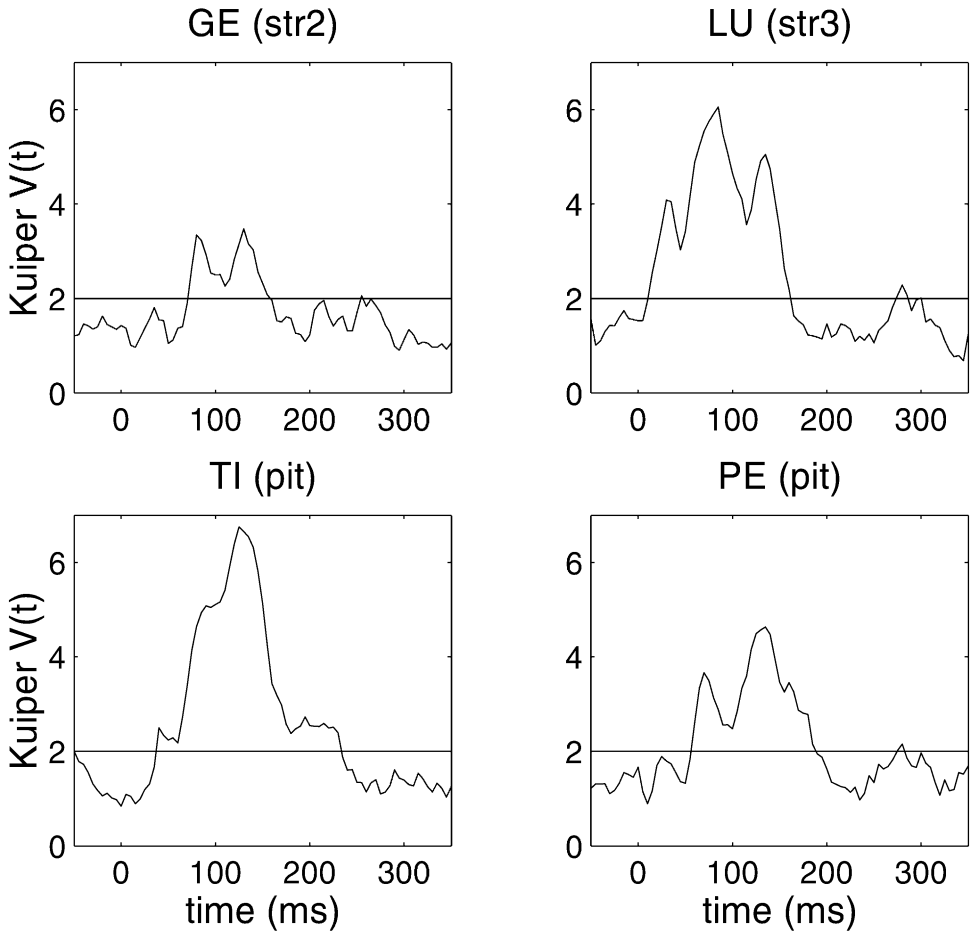

Fig. 6. Four representative Kuiper V time functions. Notice that during the pre-stimulus period, the absolute phase distributions of the 12 Hz Fourier component is not significantly different from uniform. During the evoked response, the distributions depart significantly from the uniform distribution. The horizontal line represents the critical level $V_c = 2.0$. Stimulus onset is at time 0 ms. The phase of the 12 Hz component was obtained by applying FFT on data segments from a moving window centered at time t.

ence time function during the post-stimulus period. Those peaks tended to coincide with 12 Hz peaks in the power spectrum time function of at least one of the two channels contributing to the coherence. As shown in the beginning of this section, power peak times were correlated with changes in the ensemble variance time function and AERP. Fig. 10 illustrates the relation between power and coherence peaks at 12 Hz. Second, since the computation of the spectral quantities required time segments of about 50 ms or longer, the coherence time function resembled a smoothed version of the cross-correlation time function (Fig. 11). Thus, although modulation in the coherence time functions clearly occurred, the relation between the peaks in coherence and the extrema of the AERP or the peaks in variance, was not always as evident.

3.3. Trial-to-trial variability removal and its effect on the statistical measures

We next estimated the evoked response on a single trial basis, and then formed a new residual time series by subtracting that estimated evoked response from the corresponding trial (see Section 2.2.7). This allowed further confirmation of the signal-to-noise ratio effect by testing whether the temporal modulation of the statistical measures computed on this new residual time series was significantly attenuated or removed. Fig. 12 illustrates the result of this procedure when only amplitude variability was incorporated in the model. It is evident that most of the event-related modulation of the ensemble variance has been removed. Similar results were obtained for most channels and subjects. Additional reduction of this modulation was obtained by also estimating the single trial latency of the evoked response. Fig. 13 shows that event-related modulation of the ensemble variance time functions is almost entirely removed using a model that takes into account both amplitude and latency variability of the evoked response. An exception to this result is seen by the remaining peak in the variance function of subject GE. This occurred because different parts of the AERP can have different latency variability, thus requiring a more sophisticated estimation procedure than that employed here.

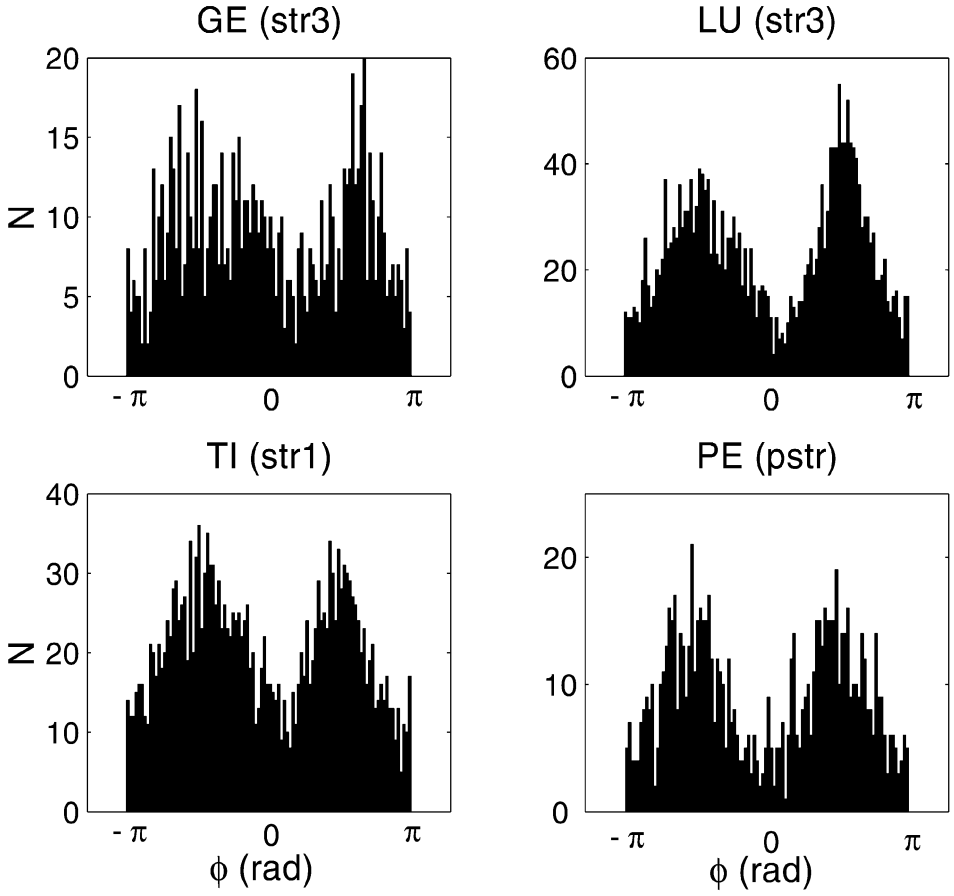

Fig. 7. Four representative examples of absolute phase distributions of the Fourier component at 12 Hz (see Section 2.2.4.), computed from a time window centered at the times 95 ms (GE), 80 ms (LU), 80 ms (TI) and 75 ms (PE) during the evoked response period. The modes of the distribution are separated by approximately π radians, as expected from the VSPN model having amplitude variability as the main factor in the trial-to-trial variability of the evoked responses. The dispersion around the modes depends on the signal-to-noise ratio of the stimulus phase-locked component in the residuals and also on the latency variability of the evoked response.

Theoretical considerations described in Section 2 show that temporal modulation of the ensemble variance underlies temporal modulation of interdependence measures. Thus, once event-related modulation of the variance time function has been removed or highly attenuated from the LFP time series of all channels, the time-dependent signal-to-noise ratio effect on the interdependence measures should also be significantly reduced. Evidence of this is seen in the coherence time functions for the 12 Hz component. Histograms of maximum coherence values during the post-stimulus period (0–200 ms) were computed for all channel pairs for each subject, both on the original residual time series ensembles and on the new residual ensembles, i.e. the single trial-evoked-responses subtracted time series. The results are shown in Fig. 14. In summary, with the original residual time series, 88% (GE), 71% (LU), 65% (TI) and 53% (PE) of the post-stimulus (0–200 ms) coherence maxima for each channel pair are greater than 0.1, compared to only 9% (GE), 5% (LU), 6% (TI) and 18% (PE) for the coherence maxima computed on the new residual time series ensembles.

4. Discussion

4.1. Variability of cortical recordings

In the traditional SPN model, trial-to-trial variability is entirely attributed to independent ongoing activity, with which a repeatable (trial-to-trial stationary) evoked response is linearly combined. The assumptions of linear combination and trial-to-trial stationarity have often been questioned in the past: non-stationarity of the evoked response has been considered as another possible source of variability in EEG and LFP recordings, while multiplicative effects between ongoing and evoked activities have been treated as leading to transient modulation of both of their variances. Substantial experimental support for variability of the evoked response, including amplitude, latency and even waveform variability, has been provided in previous studies (Coppola et al., 1978; Horvath, 1969; Lange et al., 1997; Mocks et al., 1987; Woody, 1967). The issue of whether the neural system behaves in a linear regime during the evoked response has been more controversial, with experimental

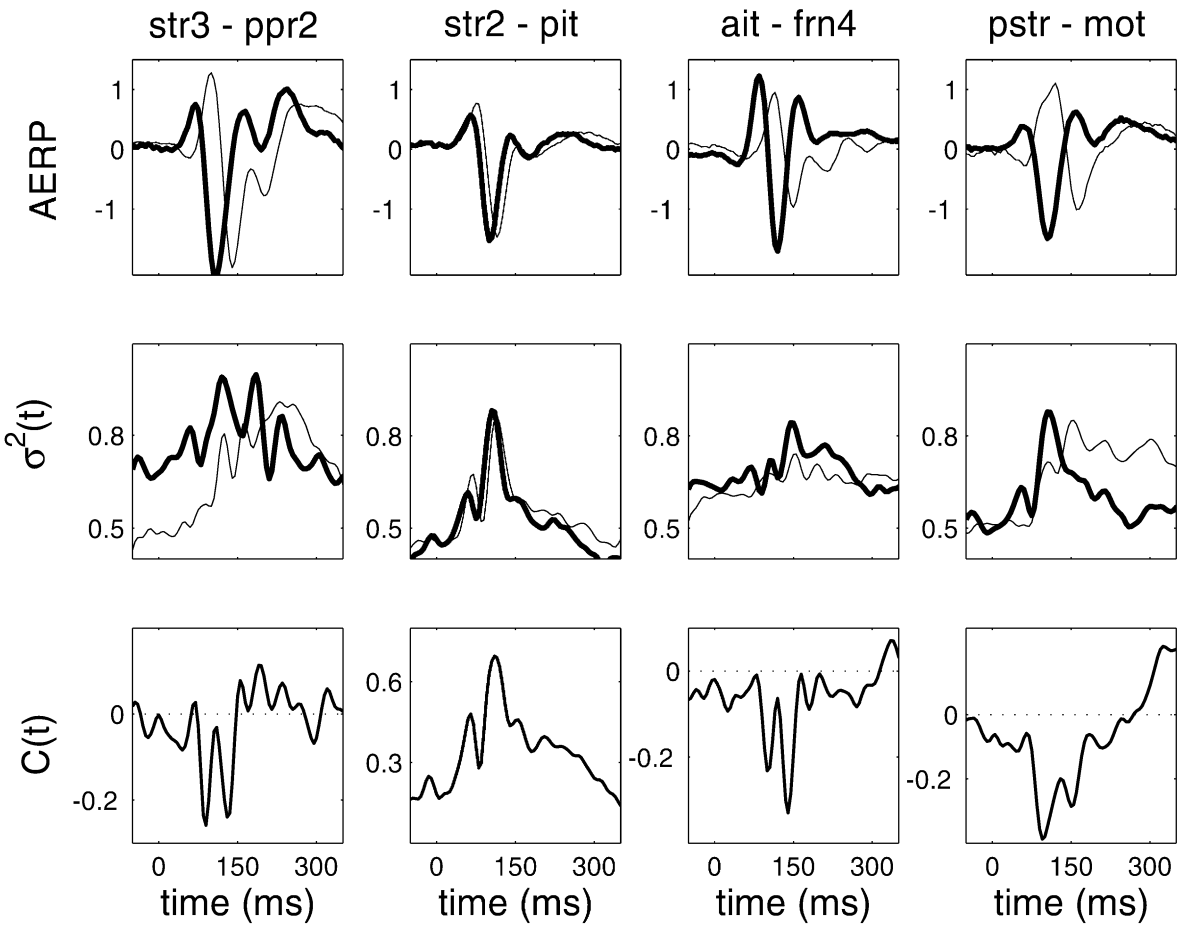

Fig. 8. Oscillatory modulation of cross-correlation time functions. Illustrative examples of zero-lag point-by-point cross-correlation coefficients from 4 channel pairs are shown (bottom row) with the respective channels AERPs (top row) and ensemble variances (center row), for 4 monkeys (from left to right: GE, LU, TI and PE). The variance was computed from low-pass filtered (−3 dB at 22 Hz), AERP-subtracted, and variance-normalized time series. Stimulus onset is at time 0 ms. The period of the oscillations in both variance and cross-correlation functions corresponds approximately to half the period of the main characteristic oscillation of the AERPs. Furthermore, peaks in variance of at least one of the channels in the pair and extrema in cross-correlation tend to coincide in time.

evidence either supporting or contradicting the linearity assumption (Aertsen et al., 1994; Arieli et al., 1996; Azouz and Gray, 1999; Chawla et al., 2000; Kisley and Gerstein, 1999; Vijn et al., 1991).

As a first refinement of the SPN model, the VSPN model assumes that the stimulus-evoked response has a stereotyped waveform but that the amplitude and latency of this waveform can vary from trial to trial. A number of possible factors may contribute to this trial-to-trial variability. For example, slow changes of global brain state involving arousal and attention could lead to fluctuations in the excitability of cortical and subcortical neuronal populations, thereby causing variability in the magnitude and timing of the evoked response (Brody, 1998; Mangun and Hillyard, 1991), without significantly affecting the shape of the response. Also, in the context of visual evoked responses, eye movements could change the location of retinal stimulation and consequently the location of cortical excitation in retinotopically organized areas (Gur et al., 1997), contributing to variability of the recorded activity from fixed electrodes. Trial-to-trial variability could also be related to the previously observed dependence of single trial evoked response amplitude on the level of pre-stimulus ongoing activity (Basar et al., 1976, 1998; Brandt and Jansen, 1991). Although all these sources of variability are commonly considered to be a violation of the stationarity assumed in ideally controlled experimental designs (Aertsen et al., 1989), we argue that some of them, like state dependent neural excitability, constitute in practice an inevitable aspect of multi-trial experiments, even for situations where the recording session might last only a few minutes.

4.2. Observed effects of the trial-to-trial variability on recorded local field potentials

Analysis of the local field potential data was intended to verify the predicted effects of trial-to-trial variability of the evoked response in a very common type of experimental design. Several lines of evidence for amplitude variability were: (1) the predicted relationship between variance and

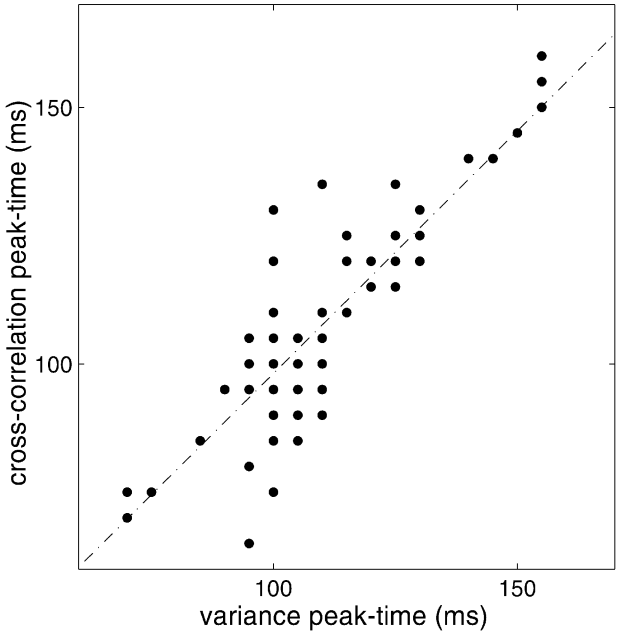

Fig. 9. Peak-time of the lagged point by point cross-correlation time function versus the peak-time of the variance function for the channel with the earliest peak in variance in the pair (see Section 2 and text). Data from 144 channel pairs selected from the 4 monkeys are shown (see text). Because of the time resolution employed (sampling interval of 5 ms), many points are superimposed. The dashed line is given from the least square linear fit (slope equal to 0.94). The VSPN model predicts a slope close to 1 for the case where amplitude variation is the key factor for the temporal modulation in the signal-to-noise ratio.

AERP waveform; (2) the bimodal histograms for phase of the 12 Hz Fourier component computed on residual time series; and (3) the diminished temporal modulation in ensemble variances after removal of single trial evoked responses. In all four subjects, the majority of recorded channels showed phase distributions that, according to the Kuiper *V* statistics, departed from uniformity, supporting the existence of stimulus phase-locked signals in the residual time series. This effect was observed during the initial period of the evoked response (50–200 ms) in almost all of the recorded cortical regions, from the primary visual cortex to the motor and frontal cortices (Fig. 6). Visual inspection of the non-uniform distributions showed them to be clearly bimodal (Fig. 7). This implies that the signal-to-noise ratio was high and that the latency variability was not severe. Large latency variability would lead to broader modes in the phase distribution. In extreme cases, the distribution would look uniform. Low signal-to-noise ratios would result in the distributions being dominated by the 12 Hz component of the ongoing activity, which again would be expected to be uniform.

The VSPN model predicted that peaks in the ensemble variance should coincide in time with extrema of the AERP for cases where amplitude variability is the main contributing factor (see Eq. 2.8). Examination of the data revealed this to be approximately the case, especially for AERP extrema before 150 ms (Figs. 4 and 5). Deviations from this prediction possibly arose because of substantial latency variability. Analysis of the power spectrum time function revealed that the main increase in variance occurred for Fourier components around 12 Hz, which was the main characteristic frequency of the AERPs (Figs. 4, 10 and 11). After subtracting single trial amplitude-estimated evoked responses from the data, we obtained removal of most of the observed temporal modulation on ensemble variance (Fig. 12). For most of the channel recordings, complete removal was obtained by estimating both the amplitude and latency (Fig. 13). These results indicate that trial-to-trial variability in amplitude was indeed the main contributor to temporal modulation of the variance and the 12 Hz power, followed by a smaller contribution from latency variability.

Regarding interdependence measures, i.e. cross-correlation and spectral coherence time functions, the VSPN model's main implication was described in terms of a time-dependent signal-to-noise ratio effect. Two main scenarios were described in Section 2.1.2. First, if the trial-to-trial amplitudes or latencies of the evoked responses recorded from two channels co-vary, the time-dependent signal-to-noise ratio effect implies that characteristic transient increases in the cross-correlation should be observed during the evoked response period. In the second scenario, the trial-to-trial amplitudes or latencies do not co-vary, but the pre-stimulus ongoing activity is correlated between the two channels. In this case, instead of a transient increase in the cross-correlation, as compared to the pre-stimulus period, a decrease should be observed. The experimental results presented in this paper related exclusively to the case of increase in cross-correlation and coherence. As expected, event-related transient increases in variance and in 12 Hz power were accompanied by transient increases in cross-correlation and 12 Hz coherence time functions for many channel pairs (Figs. 8–11 and 14). The most definite evidence for the hypothesis of trial-to-trial co-variation of stimulus time-locked components in the residual time series was the great reduction in 12 Hz coherence values of the single trial evoked response removed time series as compared to the original residuals (Fig. 14).

The coherence values[2] that remained above 0.1 for the new residual time series may still have been due to the time-dependent signal-to-noise ratio effect. For example, consider that two parietal sites receive a common input from a striate site, and moreover, that the evoked responses in both parietal sites are dominated by components other than the common one from the striate input. In this case, the single trial estimation might not capture the common striate component in the parietal recordings. The trial-to-trial variability of this component would affect the interde-

[2] Our experience with assessing the statistical significance of coherence values through bootstrap methods in this data set suggests that in general values above 0.1 are statistically significant.

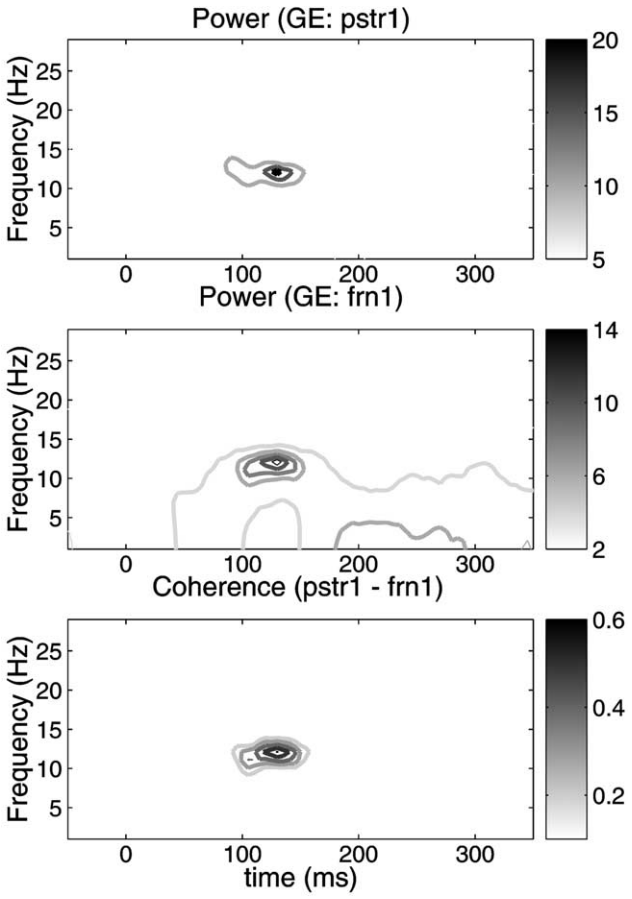

Fig. 10. Event-related changes in power and coherence spectrum time functions. In both pre-striate and frontal channels (monkey GE), the event-related changes in power and coherence concentrate around the 12 Hz component. Also, peaks in power and coherence roughly coincide in time. The spectral quantities were derived from the AMVAR modeling of the residual time series (see Section 2). Stimulus onset is at time 0 ms. Squared coherence values are used.

pendence measures, even after subtraction of the estimated single trial evoked responses. Thus, with the application of the current estimation algorithm, it is not yet possible to completely remove the time-dependent signal-to-noise ratio effect. However, the available evidence strongly suggests that the effect is indeed the main contributor to the observed event-related modulation of interdependence in this data set.

The relation between variance peak times and cross-correlation peak times (Fig. 9) was nearly linear with slope close to one, supporting the hypothesis of amplitude co-variation. Observed deviations may have originated again from latency variability or from two other factors. A complete coincidence between the peak times would be observed if the AERPs of different channels were identical, which was not the case (see Section 2.1.2 and Fig. 2). In the scatter plot (Fig. 9), many channel pairs were grouped together. Some of these channels may have had their statistical interdependence arising from higher order interactions (e.g. indirect interaction through one or more cortical areas). As in the hypothetical example of two parietal channels given above, even though a common striate input might be the main factor contributing to the modulation of their interdependence, it might only have a minor influence on the characteristic shape of their ensemble variances. In the spectral domain, a much more consistent time coincidence was observed between peaks in 12 Hz coherence and 12 Hz power (an example of this is provided in Fig. 10).

4.2.1. Possible explanations of event-related modulation of statistical quantities computed on residual time series

Power spectral density, cross-correlation and coherence functions are quantities computed on residual time series, i.e. on time series from which the average event-related potential (AERP) has been removed. Several explanations have been proposed to account for event-related temporal modulation of these measures. Perhaps the simplest source of such effect in pairwise measures is a common input to the two neuronal populations. If temporal fluctuations in the input itself are event-dependent, the statistical measures should show transient changes. A more complex mechanism would involve non-linear interaction between the populations. In this case, the assumption of linear combination of the stimulus evoked response and ongoing activity does not hold because the ongoing component could modulate, and be modulated by, the stimulus-evoked response. A simple illustration is provided in the following scenario. Dynamical

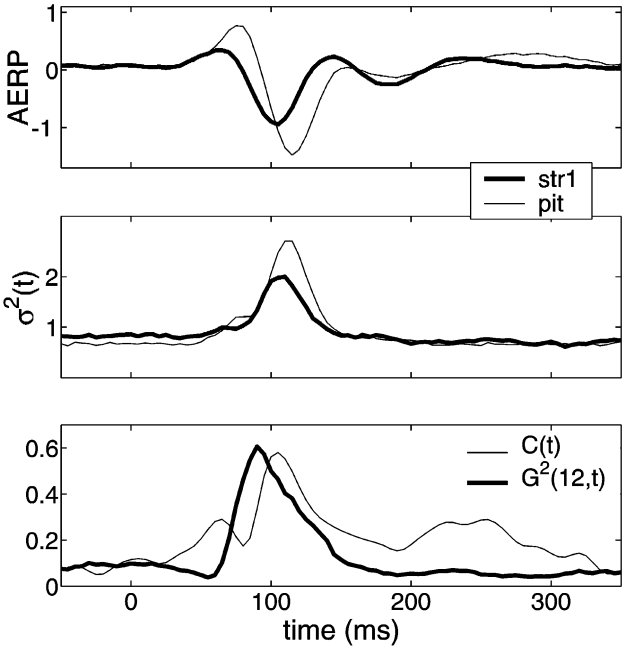

Fig. 11. The time-dependent signal-to-noise ratio effect on the coherence time function. The shape of the zero-lag cross-correlation $C(t)$ is clearly related to the ensemble variance and AERPs. The squared coherence time function of the 12 Hz component $G^2(12,t)$ resembles a smoothed version of the cross-correlation time function because of its computation within a time window. The plotted quantities refer to striate and posterior inferior temporal sites (monkey LU).

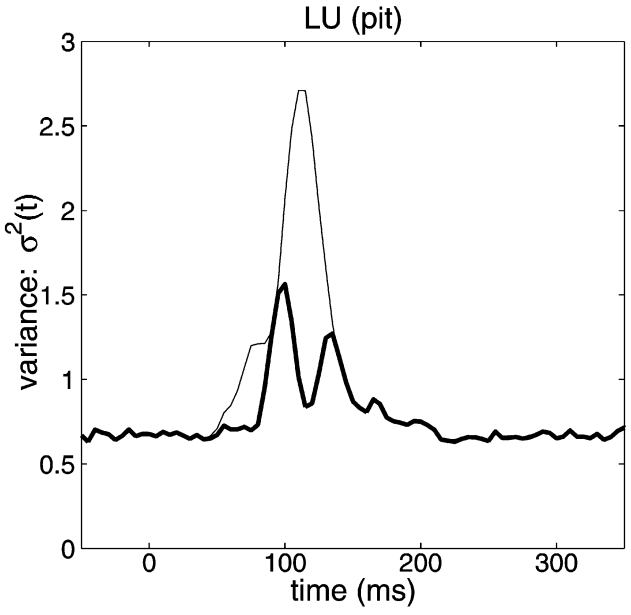

Fig. 12. Amplitude variability effect on ensemble variance time functions. The ensemble variance time function from LFP time series recorded from a posterior inferior temporal site (pit) from subject LU is shown by the thin curve. After the evoked response, scaled by the single trial estimated amplitude, has been subtracted from the corresponding single trial data, the resulting ensemble variance (thick curve) shows significantly decreased peaks. This result gives further support for the hypothesis that the trial-to-trial amplitude variability is a major contributor to the event-related modulation of the variance. Variance values were computed on normalized time series (see Sections 2.2.2 and 2.2.7).

models of neuronal population activity relate the field potential and pulse density (the number of spikes per unit volume) by a non-linear sigmoid function (Eeckman and Freeman, 1991; Freeman, 1975). A resulting property of networks of such populations is the dynamic modulation of gain and effective connectivity by the network's mean activity level (Truccolo et al., 2000, 2001). This modulation can affect both the local population properties and the interactions among local populations. First, transient changes in the population's mean level of activity, like that produced by stimulus-evoked responses, can change the gain of the population's output sigmoid function, resulting in amplification or attenuation of its ongoing activity. This effect can be measured by transient changes in the time course of the ensemble variance time function, $\langle[\eta^r(t)]^2\rangle$, and in power spectrum density time functions of the residual time series, $\langle|\eta^r(f,t)|^2\rangle$. Such changes are likely to be observed over a range of frequencies, especially if the pre-stimulus activity is broadband. Second, as the gain level of the output sigmoid function of a population changes, its effective connectivity with other populations may also be modulated, leading to possible changes in the level of synchrony between the neuronal population activities. In this way, the residual time series from two interacting populations can exhibit event-related modulation of their statistical interdependence, as measured by fast transients in the time course of cross-correlation and coherence time functions. Other non-linear mechanisms, based on the effect of the background level of activity and evoked transients on effective connectivity (Aertsen et al., 1994, 1989; Chawla et al., 1999a, 2000; Friston, 2000) are similar in spirit. Changes in intrinsic parameter regulating the frequency characteristics of neuronal populations could also lead either to resonance or to decoupling between the populations (Baird and Eeckman, 1993; Hoppensteadt and Izhikevich, 1999; Izhikevich, 1999), producing similar event-related modulations in interdependence measures.

The VSPN model considered here provides yet another possible mechanism. The residual time series contain two components: the stimulus phase-locked component and the ongoing component. Since the variance of the residual phase-locked component is modulated by the AERP magnitude, its strength relative to the ongoing component, as measured by the signal-to-noise ratio $\sigma_S^2(t)/\sigma_\xi^2(t)$, is modulated in a similar way (Eqs. (2.9) and (2.16)). When the ratio is high, the signal stands more above the noise background compared to when the ratio is low. Temporal fluctuations in this ratio give rise to modulation of interdependence measures if the amplitudes of the phase-locked components from two different channels co-vary and/or if the channels' ongoing activities are themselves correlated (as implied by

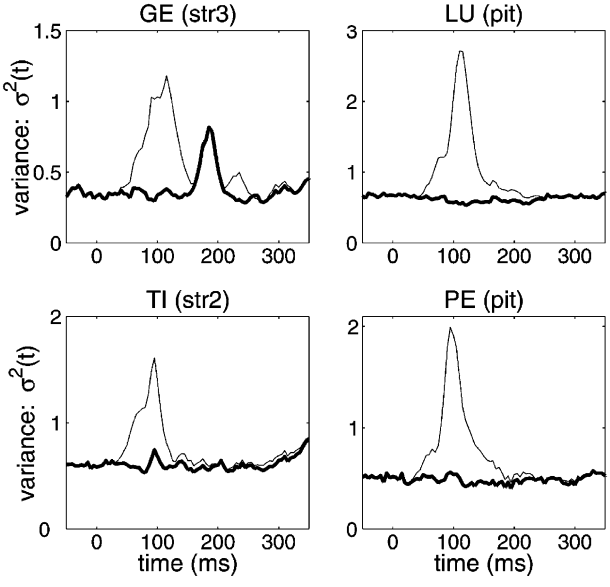

Fig. 13. Trial-to-trial variability effect on ensemble variance time functions. Examples of event-related modulation of the ensemble variances from 4 cortical sites of 4 subjects are shown by the thin curves. After the estimated single trial evoked response has been subtracted from the time series, approximately all the event-related modulation of the variance time functions has also been removed (thick curves). Here both the amplitude and latency of the evoked response were estimated following a Bayesian approach (see Section 2.2.7). The amplitude variability together with the latency variability seem to be the two major contributors to the event-related modulation of the variance, with the amplitude contributing most significantly (compare LU (pit) in this figure to that in Fig. 12). Ensemble variances were computed on normalized time series.

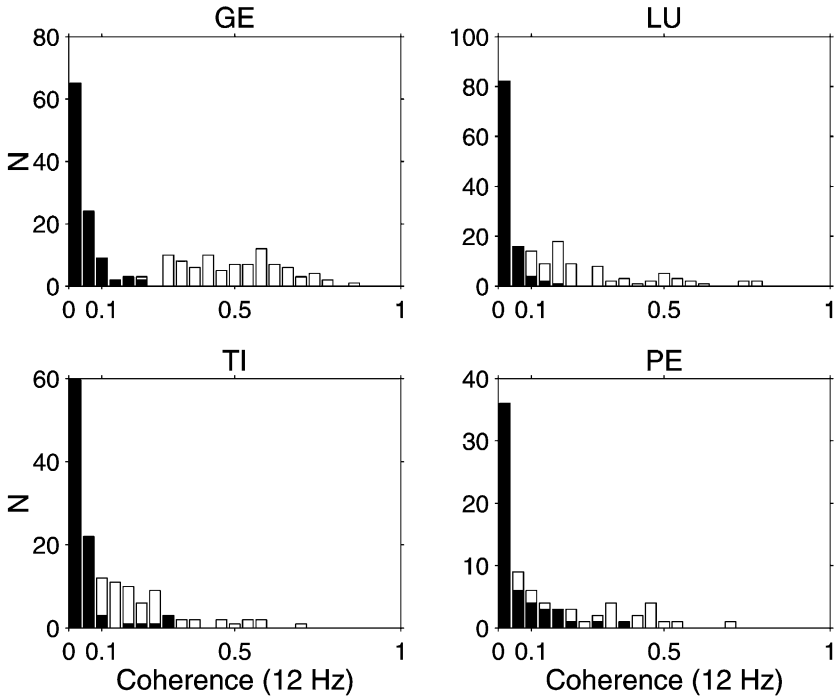

Fig. 14. Removal of the trial-to-trial variability effect on the coherence time functions. Each plot shows the maximum coherence value histograms during the post-stimulus period (0–200 ms) for all the channel pair combinations from a single subject. Histograms were computed on the original residual time series ensemble (open bars) and on the new residuals, i.e. the single trial-evoked-response subtracted time series ensemble (solid bars). As can be seen, after the single trial responses have been subtracted from the time series, the majority of the coherence maximum values are close to zero. Squared coherence values were employed.

Eqs. (2.17) and (2.19)). Similar relations between trial-to-trial variability in excitability and temporal modulation of cross-correlation have previously been investigated in spike train recordings (Baker et al., 2001; Brody, 1999; Friston, 1995). Although the trial-to-trial variability of amplitude and latency seems to be a ubiquitous characteristic of different types of recordings, including non-invasive EEG and MEG measures, the strength of the effect of this variability on statistical measures may vary depending on the type of the recordings. The crucial aspect is the level of signal-to-noise ratio. We expect that the higher this ratio, the stronger the effect of the trial-to-trial variability of evoked responses on the temporal modulation of power and interdependence measures. In this way, the effect in non-invasive recordings should present the same qualitative properties but be weaker compared to intra-cortical and sub-dural LFP recordings.

4.2.2. Separation of stimulus phase-locked and non-phase-locked components in cortical recordings

Event-related recordings commonly contain evoked and/or induced components (Freeman, 1994; Pfurtscheller and Lopes da Silva, 1999) in addition to unrelated background ongoing activities. The evoked component is usually considered to result from phase-locked responses of cortical populations to thalamic afferents, while the induced component is time-locked but not phase-locked to the stimulus, and results from transient changes in neural parameters controlling interactions among cortical populations. The evoked component tends to have a low frequency profile that can exhibit phase-locking properties in the presence of latency variability. On the other hand, induced components tend to have higher frequencies (e.g. in beta or gamma ranges) and need more careful analysis to discover. In the present work, induced activity and background activity are not differentiated and are collectively called the ongoing noise component.

Although early evoked components stemming from sensory processing (100–200 ms post-stimulus) can be separated from the ongoing activity, as our result has shown, a more difficult problem is the extraction of later evoked components, where the latency variability is larger. We know of no technique that can estimate the induced components on a trial-by-trial basis because of the lower signal-to-noise ratios. Thus more improved techniques will be required and will depend mainly on better models of evoked response and ongoing activity. For instance, the prior probabilities for the amplitudes and latencies are probably not uniform and the ongoing activity is clearly not a white Gaussian process and cannot be assumed to be stationary during the transition from pre- to post-stimulus periods (Truccolo et al., 2001). Furthermore, improved models of the evoked response signal may stipulate that, even for very localized intra-cortical LFP recordings, the evoked response is the combination of multiple and possibly overlapping components, each having its own trial-to-trial amplitude and latency variability (Gratton et al., 1989; Jung

et al., 1999; Lange et al., 1997). All these issues are fundamental for the enterprise of identifying the origins of event-related transients using statistical measures and will be addressed elsewhere (Truccolo et al., in preparation), together with the presentation of an approach for the concurrent estimation of amplitudes, latency and waveform of multi-component single trial evoked responses.

Acknowledgements

We gratefully acknowledge use of the Charles E. Schmidt College of Science computing facilities at FAU in carrying out this work. Supported by grants from NIMH (MH58190 and MH42900), NSF (IBN9723240), ONR (N0001499100 62) and a CNPq (Brazil) fellowship.

Appendix A. Bayesian estimation of single trial amplitudes and latencies of evoked responses.

A Bayesian inference framework for estimating single trial parameters is outlined in this appendix. For the special case of evoked responses that only vary in their amplitude, the problem reduces to estimating the amplitude α^r for the rth trial. Writing Eq. (2.5) in terms of discrete times, $Z^r(K) = \alpha^r E(k) + \xi^r(k)$, where k is the sample index, the posterior probability of the model parameters $\{\alpha^r\}$ and $\{E(k)\}$, given the data $\{Z^r(k)\}$, is:

$$p(\{\alpha^r\}, \{E(k)\} \mid \{Z^r(k)\}) = \frac{p(\{Z^r(k)\}|\{\alpha^r\}, \{E(k)\})p(\{\alpha^r\}, \{E(k)\})}{p(\{Z^r(k)\})} \quad \text{(A1)}$$

Note that

$$p(\{Z^r(k)\}|\{\alpha^r\}, \{E(k)\}) = \frac{(p(\{\eta^r(k)\}, \{\alpha^r\}, \{E(k)\})}{p(\{\alpha^r\}, \{E(k)\}) = p(\{\eta^r(k)\})},$$

since the ongoing activity $\eta^r(k)$ and model parameters are assumed to be independent. Assume uniform prior distributions for the model parameters. Let $\eta^r(k)$, in a first approximation, be a white Gaussian process with time independent variance σ^2. The posterior probability can then be written as:

$$p(\{\alpha^r\}, \{E(k)\}|\{Z^r(k)\}) \propto \sigma^{-NT} \exp\left(-\frac{1}{2\sigma^2}\sum_{r=1}^{N}\sum_{k=1}^{T}[Z^r(k) - \alpha^r E(k)]^2\right) \quad \text{(A2)}$$

where N and T are the number of trials and sampled data points, respectively. We chose the *Maximum a Posteriori* (MAP) solution, i.e. the amplitude estimates are chosen to be the amplitudes that maximize the posterior probability. In other words, we solve for the amplitude that makes the derivative of the logarithm of the posterior with respect to α^r equal to zero:

$$\frac{\partial}{\partial\alpha^r}\log p(\{\alpha\}, \{E(k)\} \mid \{Z(k)\} = \frac{1}{\sigma^2}\sum_{k=1}^{T} Z^r(k)E(k) - \alpha^r E^2(k) = 0 \quad \text{(A3)}$$

After a few algebraic steps, the solution is given by:

$$\alpha^r = \frac{\langle Z^r(k)E(k)\rangle_k}{\langle E^2(k)\rangle_k} \quad \text{(A4)}$$

To make the solution unique, the norm of the evoked response is constrained to equal 1. Then, the solution simplifies to:

$$\alpha^r = \langle Z^r(k)E(k)\rangle_k \quad \text{(A5)}$$

which is a matching filter solution, i.e. the dot product between the single trial recording and the normalized evoked response. Furthermore, the constraint $\alpha^r > 0$ is introduced to accommodate the known fact that the evoked response does not invert from trial to trial. For our purpose, the ensemble mean $\langle Z^r(k)\rangle$ is taken as a good estimation of the single trial evoked response $E(k)$.

This approach, as shown in Section 3.3 and Fig. 12, captures most of the single trial variability of the evoked response. Further improvement is obtained by also estimating single trial latencies. To a first approximation, a practical and easy solution in discrete time that is faithful to maximization of the posterior probability is achieved by estimating latency and amplitude variability following the three steps given in the Section 2.2.7. In those three steps, the AERP is again taken as the estimator of the evoked response $E(k)$. The resulting algorithm is similar to the Woody method for latency estimation (Woody, 1967). Related maximum-likelihood solutions have been used by Pham et al. (1987) and by Jaskowski and Verleger (1999) for the estimation of single trial latency and amplitude in the frequency domain. A more detailed treatment of the estimation issues, as well improvements on the model and procedure, are beyond the scope of the present paper and are addressed elsewhere (Truccolo, Ding, Knuth, and Bressler, in preparation).

References

Aertsen A, Erb M, Palm G. Dynamics of functional coupling in the cerebral cortex: an attempt at a model-based interpretation. Physica D 1994;75:103–128.

Aertsen A, Gerstein GL, Habib MK, Palm G. Dynamics of neuronal firing correlation: modulation of 'effective connectivity'. J Neurophysiol 1989;61:900–917.

Arieli A, Sterkin A, Grinvald A, Aertsen A. Dynamics of ongoing activity: explanation of the large variability in evoked cortical responses. Science 1996;273:1868–1871.

Azouz R, Gray CM. Cellular mechanisms contributing to response variability of cortical neurons in vivo. J Neurosci 1999;19:2209–2223.

Baird B, Eeckman FH. A hierarchical sensory-motor architecture of oscillating cortical area subnetworks. In: Eeckman F, editor. Analysis and

modeling of neural systems II, Norwell, MA: Kluwer, 1993. pp. 96–104.

Baker SN, Spinks R, Jackson A, Lemon RN. Synchronization in monkey motor cortex during a precision grip task. I. Task-dependent modulation in single-unit synchrony. J Neurophysiol 2001;85:869–885.

Basar E, Gonder A, Ungan P. Important relation between EEG and brain evoked potentials. I. Resonance phenomena in subdural structures of the cat brain. Biol Cybern 1976;25:27–40.

Basar E, Rahn E, Demiralp T, Schurmann M. Spontaneous EEG theta activity controls frontal visual evoked potentials. Electroenceph clin Neurophysiol 1998;108:101–109.

Brandt ME, Jansen BH. The relationship between prestimulus alpha amplitude and visual evoked potential amplitude. Int J Neurosci 1991;61:261–268.

Bressler SL. Large-scale cortical networks and cognition. Brain Res Rev 1995;20:288–304.

Bressler SL. Interareal synchronization in the visual cortex. Behav Brain Res 1996;76:37–49.

Bressler SL, Coppola R, Nakamura R. Episodic multiregional cortical coherence at multiple frequencies during visual task performance. Nature 1993;366:153–156.

Bressler SL, Ding M, Liang H. Investigation of cooperative cortical dynamics by multivariate autoregressive modeling of event-related local field potentials. Neurocomputing 1999;26:625–631.

Brody CD. Slow covariations in neuronal resting potentials can lead to artefactually fast cross-correlations in their spike trains. J Neurophysiol 1998;80:3345–3351.

Brody CD. Correlations without synchrony. Neural Comput 1999;11:1537–1551.

Buchel C, Friston KJ. Modulation of connectivity in visual pathways by attention: cortical interactions evaluated with structural equation modelling and fMRI. Cereb Cortex 1997;7:768–778.

Chatfield C. The analysis of time series, 4th ed. New York, NY: Chapman and Hall, 1995.

Chawla D, Lumer ED, Friston KJ. The relationship between synchronization among neuronal populations and their mean activity levels. Neural Comput 1999a;11:1389–1411.

Chawla D, Rees G, Friston KJ. The physiological basis of attentional modulation in extrastriate visual areas. Nat Neurosci 1999b;2:671–676.

Chawla D, Lumer ED, Friston KJ. Relating macroscopic measures of brain activity to fast, dynamic neuronal interactions. Neural Comput 2000;12:2805–2821.

Coppola R, Tabor R, Buchsbaum MS. Signal to noise ratio and response variability measurements in single trial evoked potentials. Electroenceph clin Neurophysiol 1978;44:214–222.

Damasio AR. The brain binds entities and events by multiregional activation from convergence zones. Neural Comput 1989a;1:123–132.

Damasio AR. Time-locked multiregional retroactivation: a systems-level proposal for the neural substrates of recall and recognition. Cognition 1989b;33:25–62.

Dawson GD. A summation technique for the detection of small evoked potentials. Electroenceph clin Neurophysiol 1954;6:153–154.

Ding M, Bressler SL, Yang W, Liang H. Short-window spectral analysis of cortical event-related potentials by adaptive multivariate autoregressive modeling: data preprocessing, model validation, and variability assessment. Biol Cybern 2000;83:35–45.

Eeckman FH, Freeman WJ. Asymmetric sigmoid nonlinearity in the rat olfactory system. Brain Res 1991;557:13–21.

Fisher NI. Statistical analysis of circular data, Cambridge, MA: Cambridge University Press, 1995.

Freeman WJ. Mass action in the nervous system, New York, NY: Academic Press, 1975.

Freeman WJ. Neural mechanisms underlying destabilization of cortex by sensory input. Physica D 1994;75:151–164.

Fries P, Reynolds JH, Rorie AE, Desimone R. Modulation of oscillatory neuronal synchronization by selective visual attention. Science 2001;291:1560–1563.

Friston KJ. Neuronal transients. Proc R Soc London Ser B, Biol Sci 1995;261(1362):401–405.

Friston KJ. The labile brain. I. Neuronal transients and nonlinear coupling. Philos Trans R Soc Lond Ser B, Biol Sci 2000;355:215–236.

Gratton G, Kramer AF, Coles MGH, Donchin E. Simulation studies of latency measures of components of the event-related brain potential. Psychophysiology 1989;26:233–248.

Gray CM. The temporal correlation hypothesis of visual feature integration: still alive and well. Neuron 1999;24:31–47.

Gray CM, Konig P, Engel AK, Singer W. Oscillatory responses in cat visual cortex exhibit intercolumnar synchronization which reflects global stimulus properties. Nature 1989;338:334–337.

Gur M, Beylin A, Snodderly DM. Response variability of neurons in primary visual cortex (V1) of alert monkeys. J Neurosci 1997;17:2914–2920.

Haykin S, Kesler S. Prediction-error filtering and maximum-entropy spectral estimation. In: Haykin S, editor. Topics in applied physics: nonlinear methods of spectral analysis, New York, NY: Springer, 1983. pp. 9–70.

Hoppensteadt FC, Izhikevich EM. Oscillatory neurocomputers with dynamic connectivity. Phys Rev Lett 1999;82:2983–2986.

Horvath RS. Variability of cortical auditory evoked response. J Neurophysiol 1969;32:1056–1063.

Izhikevich EM. Weakly connected quasi-periodic oscillators. FM interactions, and multiplexing in the brain. SIAM J Appl Math 1999;59:2193–2223.

Jaskowski P, Verleger R. Amplitude and latencies of single-trial ERP's estimated by a maximum-likelihood method. IEEE Trans Biomed Eng 1999;46:987–993.

Jung T-P, Makeig S, Westerfield M, Townsend J, Courchesne E, Sejnowski TJ. Analyzing and visualizing single-trial event-related potentials. Advances in Neural Information Processing Systems (NIPS), Cambridge, MA: MIT Press, 1999 p. 118–24.

Kalcher J, Pfurtscheller G. Discrimination between phase-locked and non-phase-locked event-related EEG activity. Electroenceph clin Neurophysiol 1995;94:381–384.

Kisley MA, Gerstein GL. Trial-to-trial variability and state-dependent modulation of auditory-evoked responses in cortex. J Neurosci 1999;19:10451–10460.

Lange DH, Pratt H, Inbar GF. Modeling and estimation of single evoked brain potential components. IEEE Trans Biomed Eng 1997;44:791–799.

von der Malsburg C. The correlation theory of brain function. In: Domany E, van Hemmen JL, Schulten K, editors. Models of neural networks II, New York, NY: Springer, 1994. pp. 95–119.

Mangun GR, Hillyard SA. Modulations of sensory-evoked brain potentials indicate changes in perceptual processing during visual spatial priming. J Exp Psychol Hum Percept Perform 1991;17:1057–1074.

McGillem CD, Aunon JI. Analysis of event-related potentials. In: Gevins AS, Remond A, editors. Methods of analysis of brain electrical and magnetic signals. EEG Handbook, Amsterdam: Elsevier, 1987 (chap 5).

Mocks J, Gasser T, Tuan PD, Kohler W. Trial-to-trial variability of single potentials: methodological concepts and results. Int J Neurosci 1987;33:25–32.

Olshausen BA, Anderson CH, Van Essen DC. A neurobiological model of visual attention and invariant pattern recognition based on dynamic routing of information. J Neurosci 1993;13:4700–4719.

Pfurtscheller G, Lopes da Silva FH. Event-related EEG/MEG synchronization and desynchronization: basic principles. Clin Neurophysiol 1999;110:1842–1857.

Pham DT, Mocks J, Kohler W, Gasser T. Variable latencies of noisy signals: estimation and testing in brain potential data. Biometrika 1987;74:525–533.

Rodriguez E, George N, Lachaux J-P, Martinerie J, Renault B, Varela FJ. Perception's shadow: long-distance synchronization of human brain activity. Nature 1999;397:430–433.

Sporns O, Tononi G, Edelman GM. Reentry and dynamical interactions of

cortical networks. In: Domany E, van Hemmen JL, Schulten K, editors. Models of neural networks II, New York, NY: Springer, 1994. pp. 315–341.

Srinivasan R, Russell DP, Edelman GM, Tononi G. Increased synchronization of neuromagnetic responses during conscious perception. J Neurosci 1999;19:5435–5448.

Tallon-Baudry C, Bertrand O, Delpuech C, Pernier J. Oscillatory gamma-band (30–70 Hz) activity induced by a visual search task in humans. J Neurosci 1997;17:722–734.

Tallon-Baudry C, Bertrand O, Peronnet F, Pernier J. Induced gamma-band activity during the delay of a visual short-term memory task in humans. J Neurosci 1998;18:4244–4254.

Tononi G, Sporns O, Edelman GM. Reentry and the problem of integrating multiple cortical areas: simulation of dynamic integration in the visual system. Cereb Cortex 1992;2:310–335.

Truccolo WA, Ding M, Bressler SL. Dynamical analysis of an oscillatory neural network. Proceedings of the IEEE–INNS–ENNS International Joint Conference on Neural Networks, Como, Italy. The Institute of Electrical and Electronics Engineers, Inc. 2000.

Truccolo WA, Ding M, Bressler SL. Temporal modulation of variability and interdependence of local field potentials: effects of gain modulation and nonstationarity. Neurocomputing 2001;38–40:983–992.

Vijn PCM, van Dijk BW, Spekreijse H. Visual-stimulation reduces EEG activity in man. Brain Res 1991;550:49–53.

Woody CD. Characterization of an adaptive filter for the analysis of variable latency neuroelectric signals. Med Biol Eng 1967;5:539–553.